DOCUMENTING THE OCCURRENCE OF CAROLINA BAYS ON LONG ISLAND

By Gloria Gill
Under the Supervision of Distinguished Professor Dr. Gil Hanson
Stony Brook University

Introduction

Carolina bays are elliptical to circular shallow depressions found in abundance along the Atlantic Coastal Plain. They are a characterized by a closed elevated rim and a flat bottom. Although bays vary in size, neighboring bays are consistently similar in orientation and shape to each other. The time and method of formation of these enigmatic geologic land features has been debated since the early 1940's. Prior to the advent of digital elevation maps, Carolina bays were only observable in air photos particularly in North Carolina, South Carolina and Georgia. Here the majority of the 500,000 elliptical formations were coined "bays" for the bay trees that commonly grow in them (Prouty 1952). Several hypotheses have been proposed to explain their origin and time of formation, yet none have been able to simultaneous explain all their characteristics including their raised rims, flat bottoms, perfect elliptical shapes and overlapping development. This research will not propose a method of formation but instead focuses on the documentation of Carolina bays on Long Island. The Carolina bays on Long Island are small and have either an east to west or northeast to southwest orientation and distinct a bell shape. Recent advances in digital elevation mapping called LiDar imagery has allowed for the mapping of bays on Long Island. Prior to this technology dense vegetation coupled with the development shielded bays from areal view on Long Island. The discovery of bays on Long Island is significant because it places a time constraint on the age of bay formation because Long Island is relatively young in comparison to the continental United States. Figure 1 shows a section of a DEM displaying several Carolina Bays in South Carolina, and figure 2 shows shallow depressions similar to Carolina bays found on Long Island. Observing these images, it is hard not to wonder about the obvious and consistent orientation of the major axis of each ellipse and their overlapping nature.

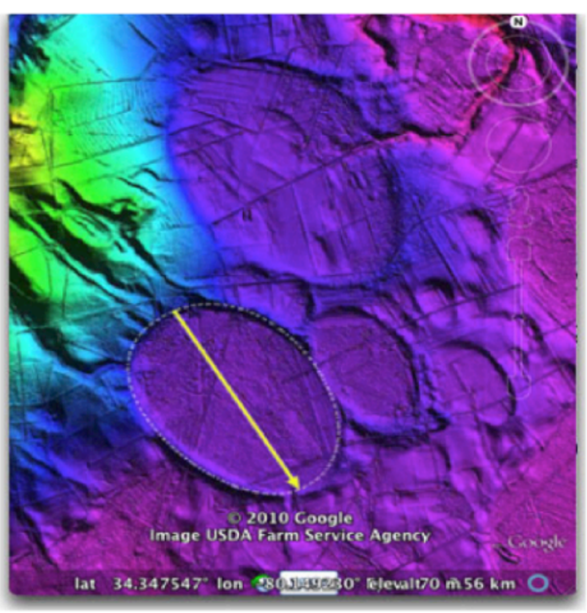

Figure 1: DEM image of Carolina bay formations in South Carolina. Note the elliptical shape, consistent orientation of the major axis, raised rims and over lapping nature.

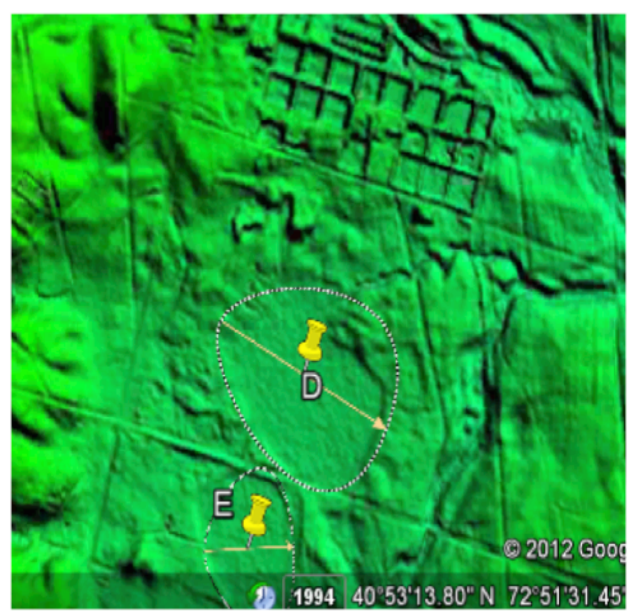

Figure 2: LiDar image documenting Carolina bays similar to those in figure 1, found on Long Island. This research discovers the presence of bay formations on Long Island, proposing a significant time constraint on the age of formation.

There are two distinct goals in documenting Carolina bays on Long Island:

The main objective of this research is to use LiDAR-derived high resolution, digital elevation maps to locate and determine the orientations of the shallow, rimmed depression on Long Island. Another interest is to produce a time constraint to the geologic event(s) or processes responsible for bay formation. Therefore this paper will discuss the unique glacial history of long island and it's youth in comparison to the main land.

The analysis of the location, size, shape and orientation of bay formations on Long Island will be used to test the hypothesis that bay formation are the remnants of an ancient cosmic collision. This paper will discuss the proposed theory of an extraterrestrial impact 12,900 years ago that may have contributed to the mega faunal extinctions and the Younger Dryas cooling and how the presence of bay formations on Long Island may help support this theory. Future research analyzing substrate characteristics, along with other identifying features of bays, may clarify the role of several erosional processes in forming these particular depressions on Long Island.

History of proposed methods of the formation of the Carolina bays:

The proposed mechanisms for bay formation include one or a combination of several erosional agents such as wind, substrate dissolution, meteorite impacts or marine waves and currents (Davias, 2010). This paper will discuss three of the leading proposals of formation.

Hypothesis 1) Carolina bay formations are the result of a combination of eolean and wave erosional processes that occur not as a single event but over an accumulation of time. In 1970, Thom associated the sandy substrates of the Carolina bays with water filled depressions usually found within dune fields. He argues that the elongated morphology is the result of wave erosion and subsequent deposition of the rims. Field research conducted during the 1980s and 1990s in South Carolina, North Carolina, Virginia and Maryland agree that bay formations are not the product of a single event but rather develop and evolve over time due to strong erosional forces including wave action and eolean processes (Gamble et al., 1977; Bliley and Pettry, 1979; Stolt and Rabenhorst, 1987a; Bliley and Burney, 1988; Carver and Brook, 1989; Markewich and Markewich, 1994; Grant et al., 1998; Ivester et al., 2007). Further studies in the late 1990's support this thesis as well. Using GPR surveys, cores, radiocarbon dates and stratigraphy, Brooks (1996) and Grant (1998) conclude that fluctuating lake levels, wave action, and parabolic-dune accretion are a part of a multi-stage rim accretion process. They also support Thom in that the near shore zone is the sediment source for the raised rims and therefore a water filled basin must first exist prior to the rim accretion. Grant et al (1998) does not address the initial basin formation but rather focuses on the rim depositional processes believed to have occurred post the Younger Dyras during the Holocene (Rodriguez, 2012). Both hypotheses Thom (1970) and Grant et al. (1998) do not propose a method nor time constraint for the basin formations.

Hypothesis 2) Carolina bays are karst like depressions due to substrate dissolution during periods of low sea level. In 1999, May and Warne argued that the formations found in the Carolinas were karst-like depression resulting from the dissolution of iron-oxide, extensive alteration of kaolinite to gibbsite and the desilicification of the sandy and clayey substrates beneath the bays. They propose that this occurred during the common low sea and water table levels of the Pleistiocene and that wind and ice further shaped the bays until the subsequent rise in sea level during the Holocene (May, 1999). Although this proposal adequately explains how substrate dissolution could form a depression, it fails to offer an explanation to the orientation or raised rims of the Carolina bay formations. In order for this hypothesis to hold substrate on long island must be rich in Kaolinite.

Hypothesis 3) Carolina bays are remnants of a cosmic collision. Cintos researcher Michael Davias used LiDAR digital elevation maps and Google Earth to study the circumferal rims and orientation of the shallow basins of the Atlantic coastal plain. Davias's research model is that the Carolina bays resulted from the impact of debris from an oblique cosmic collision with the Wisconsin ice sheet. (Davias, 2012) Davias believes that a large low density comet composed of hydrated silica impacted the ice sheet overlaying current day Michigan, specifically the Saginaw region and Lake Huron, see figure 3. The comet is thought to have hit on a nearly tangential angle, creating a non-typical oval crater orientated southwest to northeast, coined by Davias as the Saginaw impact structure. It is deeper toward the Northeast (Lake Huron) and characterized by an arced central ridge called Charity islands that is thought to be rebounded strata. These features (the ridge, the upward deeper excavation and oval shape) of the Saginaw crater are expected attributes of an oblique impact structure. Furthermore, he argues that the ice sheet itself protected the sedimentary strata of the Michigan basin, thus shearing the land rather than compressing it, therefore shocked quartz and other classic impact markers are not present. The impact ejected superheated ice and sediments outward in a butterfly pattern away from the site. See Figures 3 & 4. Davias argues that Carolina bays are evidence of a blanket of distal ejecta from this collision. Specifically he proposes "that shallow basins were created during the energetic deflation of gas inclusions in those superheated hydrous ejecta. The resulting paleobasins have persisted over the intervening millennia as "Carolina bays", "Rainwater Basins", "Maryland Basins", etc, while being overlain with loess and subjected to reworking by water and wind erosion." Taking into account the Coriolis effect during flight time of the ejecta and the curvature of earth, he seeks to interpolate the original impact site using bay orientation data collected from LiDAR imagery overlaying in google earth. (Davias, 2010)

Figure 3: Michael Davias's proposed location of the Saginaw Impact Stucture. Here a comet is thought to have hit the Wisonsian Ice Sheet on a nearly tangential angle. The crater is deeper toward the Northeast and characterized by an arced central ridge called Charity islands that is thought to be rebounded strata. The ice sheet itself protected the sedimentary strata of the Michigan basin, thus shearing the land rather than compressing it, therefore shocked quartz and other classic impact markers are not present.

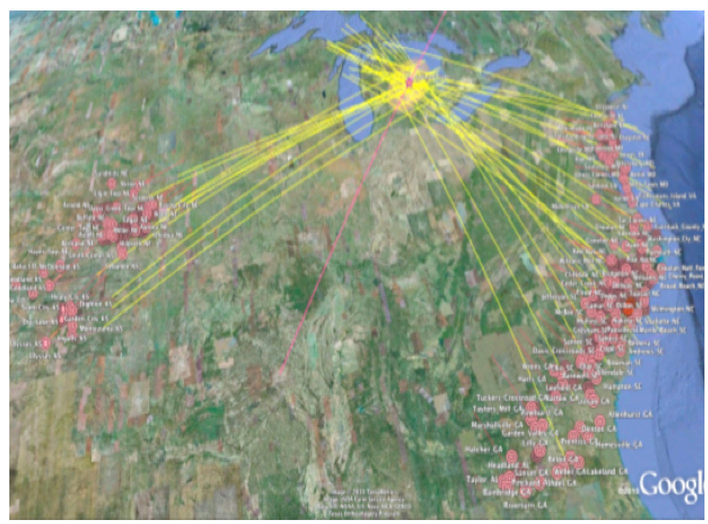

Figure 4: Researcher Michael Davias proposes that bay formations are the remnants of an ancient cosmic collision with the Wisconsian ice sheet. He hypothesizes that the impact ejected superheated ice and sediments outward in a butterfly pattern creating the shallow basins commonly know as Carolina bay formations.

Methods:

The process of identify, labeling and measuring bay formations on Long Island was adapted from Michael Davias's technique which is described in detail on his website (Davias, 2012b). Specifically, a bay formation is characterized by an elliptical shape enclosed by an elevated rim. The centers of the bays are generally flat and shallow. This distinguishes them from other surface features that look similar such as oxbow lakes and kettle holes.

The Laser Imaging, Detection and Ranging (LiDAR) mapping technique is a new advancement in digitally mapping topography. Compared to prior USGS topographic data, LiDAR data achieves much higher resolution using lasers flown over target areas, acquiring elevation data every one meter or less and elevations with uncertainties of 10's of centimters. This technique results in millions of elevation points, a level of accuracy previously unseen for elevation technologies. Furthermore, the land elevations of vegetated areas are measured that would be nearly impossible to survey with as high an accuracy by other means. (Drewberry, 2007) Like previous topographic data, in order to be accessible the LiDAR topographic data is converted into a digital elevation model (DEM). The LiDAR data gives elevation and latitude/longitude coordinates that when placed into a program, creates a DEM. The DEM uses a hue-saturation-value (hsv) to color code different elevations, such maps highlight small changes in elevations and thus accentuate the Carolina bay formations. "A digital elevation model is a representation of topography in digital format. High-resolution digital elevation models are available for the State of New York including Long Island The appearance is as if one were viewing color-enhanced images of a barren terrain, for example Mars. This allows one to see much greater detail than is possible on a standard topographic map" (Hanson, 2005). Previous technologies have a horizontal resolution of 10 meters and are based on 10-foot topographic maps, however the liDAR end product is a digital bare earth model equivalent to two foot contours with a root mean square error of only .27 feet (Drewberry, 2007). Figure 5 to the right is an example of a LiDAR derived DEM for an area in Suffolk County, New York. This higher level of detail, coupled with the availability of tools in Global Mapper ™ (Blue Marbel, 2012) to analyze three dimensional profiles of arbitrary paths and areas, allows us to make interpretations that were not possible with topographic maps alone.

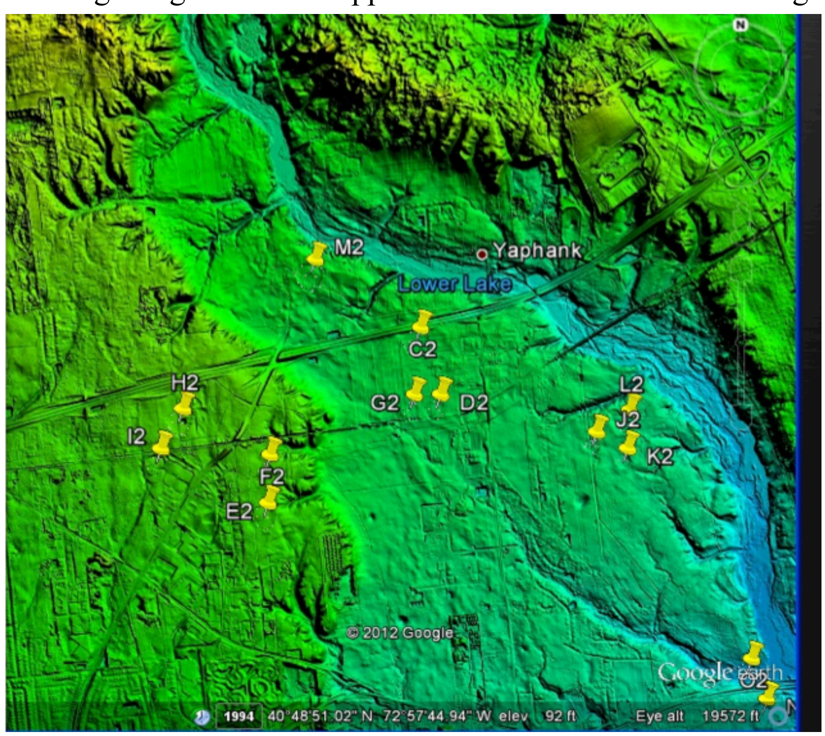

Figure 5: Example of a LiDAR derived DEM. Resolution is equivalent to a two foot contour map. LiDAR imagery was used in combination with Global Mapper and Google Earth to survey Carolina bay formations on Long Island, marked with yellow thumbtack symbols.

Mapping bay formations on long island was achieved using Google Earth and Global Mapper. First a series of octants were created in Google Earth to divide Long Island into eighteen sections by inserting rectangular polygons. Each octant covered a spatial area 1/4 degree latitude by 1/4 degree longitude. (~23 x ~27.5 km) or 1/8 th of a USGS 100K quadrant (Davias, 2012). Place marks were added to the center of each octant and labeled using the six-digit scheme developed by Davias. The first three numbers were held consistent for an entire row and increased consecutively heading north. The last three digits refer to the column and increased consecutively heading west. See figure 6 below. Adding LiDAR imagery to Google Earth was achieved using Global Mapper, a program able to open LiDar imagery files (denoted by ".avi") and convert them to KMZ files by simply using the "save as" tool. This KMZ file was simple opened in Google earth as an overlay.

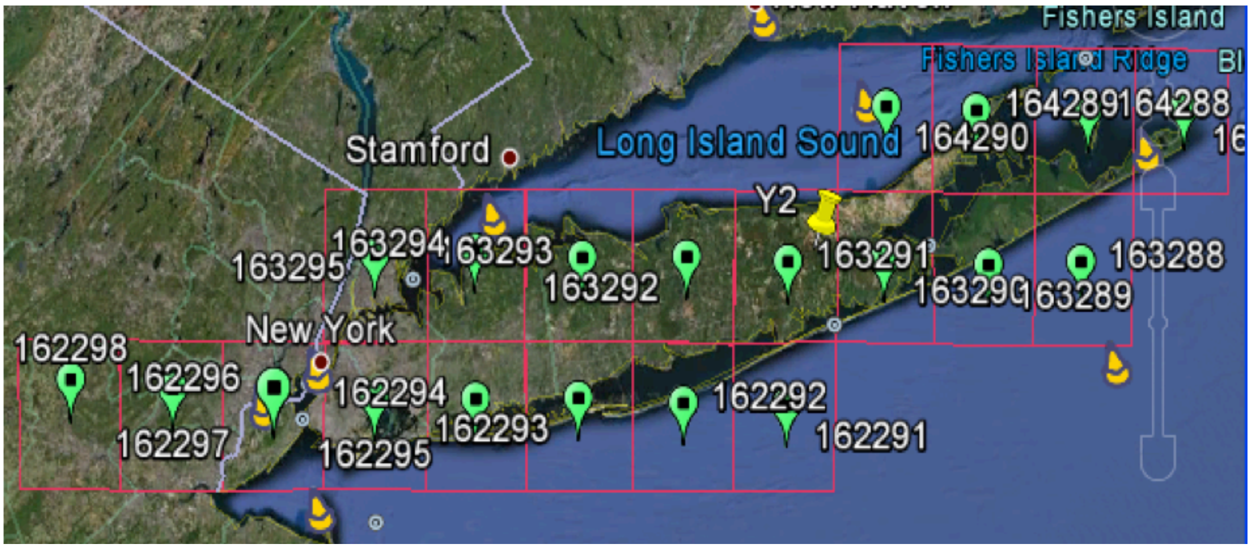

Figure 6: The first step in the research was to break Long Island, NY into eighteen Octants in Google Earth. This research documents bay formations found in octant 163291.

Although bay formations were visible on the LiDAR imagery across Long Island, Octant 163291 was chosen for this research due the heavy concentration of bay formations in this area. Most formations were found in the nature preserves and other undeveloped areas in this eastern section of Long Island. Specifically bay formations were identified in the following nature preserves.
See Figure 7.

1) The Rocky Point State Pine Barrens Preserve
2) Calverton Pond Preserve (Fox Pond, Sandy Pond, Linus Pond)
3) Wertheim National Wildlife Refuge along Carman's River
4) Southhaven County Park
5) Peconic River County Park
6) Deep Pond Nature Preserve

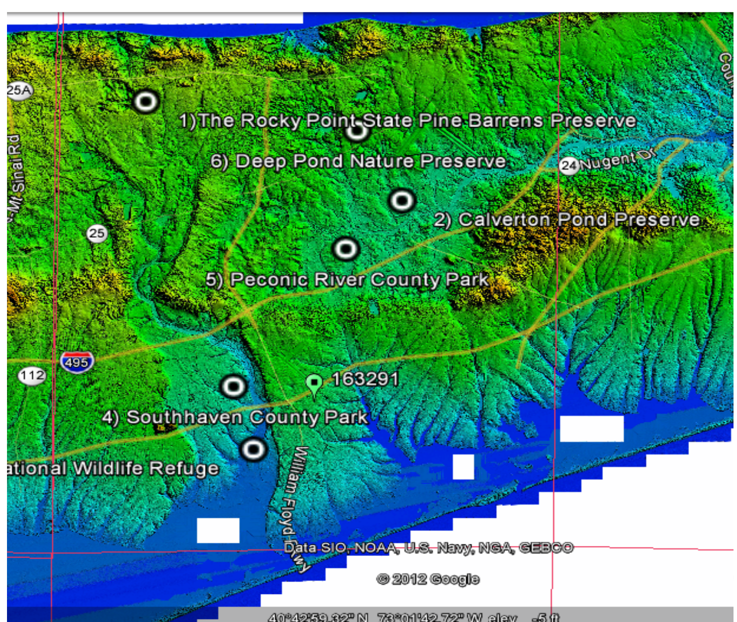

Figure 7: Close up of areas in Octant 163291 surveyed for Carolina bay formations. Symbols represent nature preserves where bays were found in their undeveloped land.

The documentation and measuring of Carolina bay formations on Long Island was achieved by adopting Davias's technique. Davias's "Carolina Bay Overlay Generation Tool" was used to generate an ellipictal overlay for placement in Google Earth, using a placemark within the bay. An overlay planform is the term that decribes the oval shaped overlay used to survey the bays. These overlay planforms are copied and edited for size and orientation within each actual bay image (Davias, 2012). After comparing bay formation in South Carolina, New Jersey and Long Island, it was determined that bay formations in Long Island were most similar to those in New Jersey. A single Carolina bay in New Jersey, already documented by Davias was chosen to serve as the model for Long Island Carolina bays. This bay's planform overlay was copied to serve as the planform overlay to capture data on the size and orientation of bays found in Long Island. In order to copy this overlay the following steps were taken.

1) The New Jersey LiDAR imagery for octant 161296 was opened in Google Earth, this file can be downloaded from the Cintos Website using the Bay Survey tab and clicking on the Overlay Generator tool. (http://cintos.org/Survey/tools/OverlayGenerator/index.html)
2) Once this octant file was open in Google earth, a bay formation was chosen to be copied. An information bubble will appear when toggling over the placemark for the bay. Here a link titled "Load Overlay for bay formation" is clicked and will appear in the DOM (document object model on the right side of the google earth screen) under temporary places.
3) The bay planform was copied and pasted into the folder for Octant 163291 by right clicking on the planform overlay.
4) In order to rename, move and resize the bay overlay, the bay was highlighted in the DOM and left clicked and the last item in the pop up: "Get Info" (Mac) or "Properties" (Win) was selected.
5) Once a green box appeared around the bay formation it was dragged to the label a bay found in Octant 163291. The bay was sized to fit appropriately and rotated to orientate the major axis. The bay was renamed " NEW 163291-A" and the information box was closed.
6) Finally this bay was right clicked in the DOM and "snap shot" view was selected to remove the attachment to the location of the original bay in New Jersey and an attach it instead to the new octant in Long Island.
7) This first bay served as the new template for labeling Long Island bays in Octant 163291. This bay was repeatedly copied, moved, renamed and adjusted by repeating steps 2 through 5.
8) A place mark was added and centered on each bay to denote each bay by a letter code.

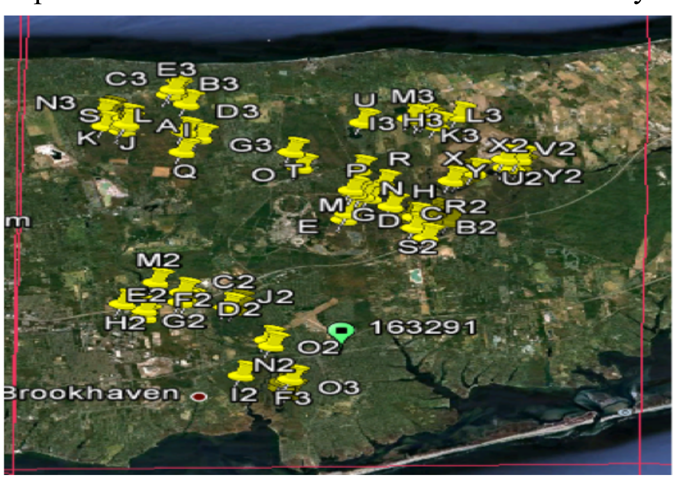

Figure 8: Close of octant 163291 and the location of 74 Carolina Bay formations.

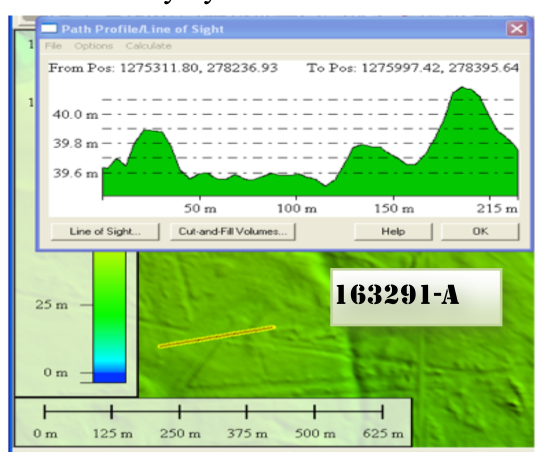

Figure 9: Analysis of a single bay labeled 163291-A. Shows both the LiDAR topographic image of the bay and a profile view along the yellow line.

A total of 74 bays were identify and labeled with a bay overlay template. Afterwards each bay was further examined using Global Mapper. The LiDAR imagery was loaded into Global Mapper and each bay was analyzed individually. This was accomplished by zooming in on a bay formation and centering it between the vertical and horizontal scales on the screen. Using the profile tool, a cross section of each bay was taken. Using the screen shot key, this data was captured along with an Arial view of the bay against the scales. The pictures were cropped and labeled as necessary and included as data in the results section of this paper. See figures 8 and 9 on the previous page.

Data:

Table 1 summarizes the measurements of Bay formations. It lists the height of the West Rim, Base & East Rim above sea-level in meters. It lists the overall orientation of the bay and the length of the axis from rim to rim. The difference between the rims and base was found for both the West and East rims of each bay. These values were subtracted to determine if there was consistency in the difference between height of each rim. Negative values indicate that the East rim is higher, where as positive values indicate that the West rim is higher.

Table 1: Bay data from Quadrant 163291. All Measurements are in meters.

Bay	West Rim elevation above Sea level (m)	Base elevation above sea level (m)	East Rim elevation above sea level (m)	Compass Orientation of major axis	Axis Length (m)	West Rim Height above Base	East Rim Height above Base	Difference in West - East height above base
A	39.9	39.5	40.2	WE	125	0.4	0.7	-0.3
B	13.5	11.3	12.75	NW-SE	300	2.2	1.45	0.75
C	15.1	13.4	15.4	NW-SE	250	1.7	2	-0.3
D	14.9	14.2	15.8	NW-SE	400	0.7	1.6	-0.9
E	14.99	14.35	14.9	NW-SE	350	0.64	0.55	0.09
F	15.4	12.4	13.6	WE	350	3	1.2	1.8
G	17.5	15.6	18	WE	275	1.9	2.4	-0.5
H	16.9	15.9	17.2	WE	270	1	1.3	-0.3
I	29.7	28.8	30.2	WE	100	0.9	1.4	-0.5
J	36.7	35.6	36.1	WE	190	1.1	0.5	0.6
K	35.8	35.2	36.9	WE	175	0.6	1.7	-1.1
L	36.9	36	36.7	WE	110	0.9	0.7	0.2
M	16.8	16.3	17.8	NW-SE	110	0.5	1.5	-1
N	18.6	17.2	18.9	NW	100	1.4	1.7	-0.3
O	22	20	25	NW-SE	140	2	5	-3
P	18.2	17.2	18.7	NW	200	1	1.5	-0.5

Bay	West Rim elevation above Sea level (m)	Base elevation above sea level (m)	East Rim elevation above sea level (m)	Compass Orientation of major axis	Axis Length (m)	West Rim Height above Base	East Rim Height above Base	Difference in West - East height above base
Q	28.6	28.1	29.9	WE	80	0.5	1.8	-1.3
R	20.6	19.4	21.4	WE	300	1.2	2	-0.8
S	36.6	35.6	36.2	WE	140	1	0.6	0.4
T	28.4	26.2	28.2	NW-SE	325	2.2	2	0.2
U	18.9	13.5	23	NW-SE	700	5.4	9.5	-4.1
V	13.9	12.2	13.9	WE	465	1.7	1.7	0
W	13	11	14.2	WE	550	2	3.2	-1.2
X	14.6	11.9	13.1	WE	260	2.7	1.2	1.5
Y	12.8	11.4	14.4	NW-SE	200	1.4	3	-1.6
Z	13.6	11.4	12.2	WE	260	2.2	0.8	1.4
A2	41.1	40.8	41.15	NW-SE	100	0.3	0.35	-0.05
B2	12.4	11.7	12.5	NW-SE	200	0.7	0.8	-0.1
C2	16.8	16.1	16.75	NW-SE	250	0.7	0.65	0.05
D2	15.5	14.8	15.4	WE	220	0.7	0.6	0.1
E2	30.5	29.9	30.5	NW-SE	300	0.6	0.6	0
F2	32.6	32	32.5	WE	150	0.6	0.5	0.1
G2	15.5	15.1	15.4	WE	150	0.4	0.3	0.1
H2	34	33	33.5	WE	270	1	0.5	0.5
I2	4.9	4.3	5	WE	125	0.6	0.7	-0.1
J2	13.5	12.7	13.6	WE	180	0.8	0.9	-0.1
K2	12.6	11.6	12.9	WE	190	1	1.3	-0.3
L2	13.9	12.3	12.9	WE	200	1.6	0.6	1
M2	19.3	17.4	18.6	WE	330	1.9	1.2	0.7
N2	7.6	6	7.1	WE	250	1.6	1.1	0.5

Bay	West Rim elevation above Sea level (m)	Base elevation above sea level (m)	East Rim elevation above sea level (m)	Compass Orientation of major axis	Axis Length (m)	West Rim Height above Base	East Rim Height above Base	Difference in West - East height above base
O2	3	2.45	2.75	WE	225	0.55	0.3	0.25
P2	13.6	12.2	13.2	WE	237	1.4	1	0.4
Q2	11.4	11.05	11.6	WE	160	0.35	0.55	-0.2
R2	13.4	12.6	15.2	WE	243	0.8	2.6	-1.8
S2	13.4	12.2	12.9	NW-SE	190	1.2	0.7	0.5
T2	13	12	13.4	WE	220	1	1.4	-0.4
U2	13.4	10.8	14.4	WE	160	2.6	3.6	-1
V2	11.8	11.1	13.1	WE	450	0.7	2	-1.3
W2	12	10.4	12.6	WE	240	1.6	2.2	-0.6
X2	12.7	11.1	11.7	WE	197	1.6	0.6	1
Y2	13.8	11.2	13.8	NW-SE	175	2.6	2.6	0
Z2	39.8	39.2	40.4	WE	130	0.6	1.2	-0.6
A3	41.6	40.8	41.7	NW-SE	253	0.8	0.9	-0.1
B3	40.3	39.8	40.7	NW-SE	200	0.5	0.9	-0.4
C3	42	41.2	42.2	WE	100	0.8	1	-0.2
D3	40.2	39.8	40.4	WE	110	0.4	0.6	-0.2
E3	41.9	41	42	WE	150	0.9	1	-0.1
F3	2.4	1.7	2.2	WE	110	0.7	0.5	0.2
G3	29.8	28.6	29.9	WE	225	1.2	1.3	-0.1
H3	29.9	28.6	29.9	WE	200	1.3	1.3	0
I3	26.8	26.3	28.8	WE	300	0.5	2.5	-2
J3	26.7	26.3	29	WE	350	0.4	2.7	-2.3
K3	18.5	14.5	18.9	WE	125	4	4.4	-0.4
L3	26.3	26.1	26.8	WE	150	0.2	0.7	-0.5

Bay	West Rim elevation above Sea level (m)	Base elevation above sea level (m)	East Rim elevation above sea level (m)	Compass Orientation of major axis	Axis Length (m)	West Rim Height above Base	East Rim Height above Base	Difference in West - East height above base
M3	25	15.6	17	WE	140	9.4	1.4	8
N3	40.2	39.3	40.2	NW-SE	170	0.9	0.9	0
O3	2.7	1.6	2.2	WE	250	1.1	0.6	0.5
P3	1.3	0.9	1.2	WE	125	0.4	0.3	0.1
Q3	1.4	1.1	1.8	WE	170	0.3	0.7	-0.4
R3	2.1	1.7	1.95	WE	125	0.4	0.25	0.15
S3	0.8	0.4	0.7	WE	150	0.4	0.3	0.1
T3	2.5	1.7	2.1	WE	125	0.8	0.4	0.4
U3	1.8	1.1	1.8	WE	130	0.7	0.7	0
V3	1.5	1.1	1.7	WE	242	0.4	0.6	-0.2
Average	20	18	20		218	1.3	1.4	-0.13
Standard Deviation	12.2	12.3	12.3		108.8	1.3	1.3	1.3

Results:

Below are 74 figures that document each individual bay formation found in quadrant 163291 (Eastern Long Island). A cross-sectional view of each bay is taken from west to east. Each bay is labeled with an alphanumeric code. Bays generally show a West to East orientation. The rims are neither higher on the west nor east side but instead show minor variation in both directions. The bases of the bays are generally flat and shallow. The bays range in size from 80 meters to 700 meters and average 218 meters across the major axis with a standard deviation of 108.9 meters. The height of the rims the base is about 1.4 meters on average with a standard deviation of 1.3 meters. Therefore the rims are comparatively small in height compared to the length of the axis. Bay formations on Long Island have more bell- shaped appearance than oval appearance. Bays tend to overlap each other and clusters of bays vary in size.

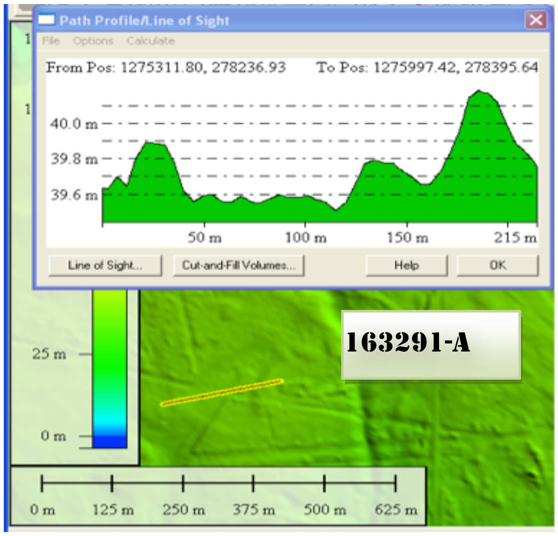
Path Profile/Line of Sight
File Options Calculate
From Pos: 1275311.80, 278236.93 To Pos: 1275997.42, 278395.64
40.0 m
39.8 m
39.6 m
50 m 100 m 150 m 215 m
Line of Sight... Cut-and-Fill Volumes... Help OK
163291-A
25 m
0 m
0 m 125 m 250 m 375 m 500 m 625 m

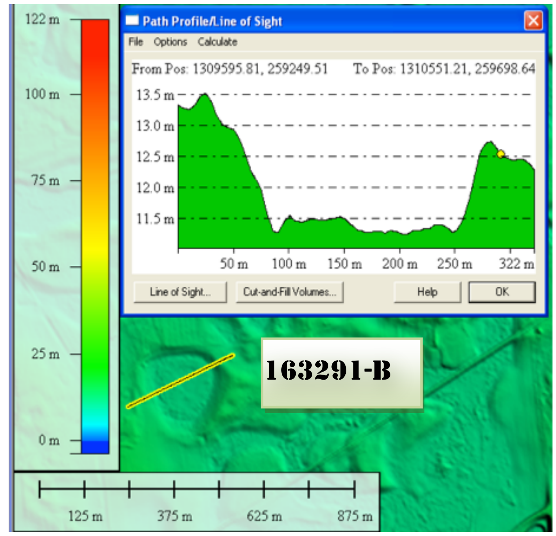
122 m
100 m
75 m
50 m
25 m
0 m
Path Profile/Line of Sight
File Options Calculate
From Pos: 1309595.81, 259249.51 To Pos: 1310551.21, 259698.64
13.5 m
13.0 m
12.5 m
12.0 m
11.5 m
50 m 100 m 150 m 200 m 250 m 322 m
Line of Sight... Cut-and-Fill Volumes... Help OK
163291-B
125 m 375 m 625 m 875 m

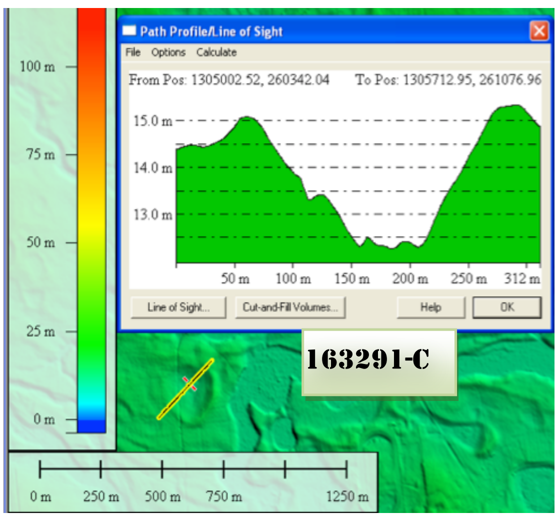
100 m
75 m
50 m
25 m
0 m
Path Profile/Line of Sight
File Options Calculate
From Pos: 1305002.52, 260342.04 To Pos: 1305712.95, 261076.96
15.0 m
14.0 m
13.0 m
50 m 100 m 150 m 200 m 250 m 312 m
Line of Sight... Cut-and-Fill Volumes... Help OK
163291-C
0 m 250 m 500 m 750 m 1250 m

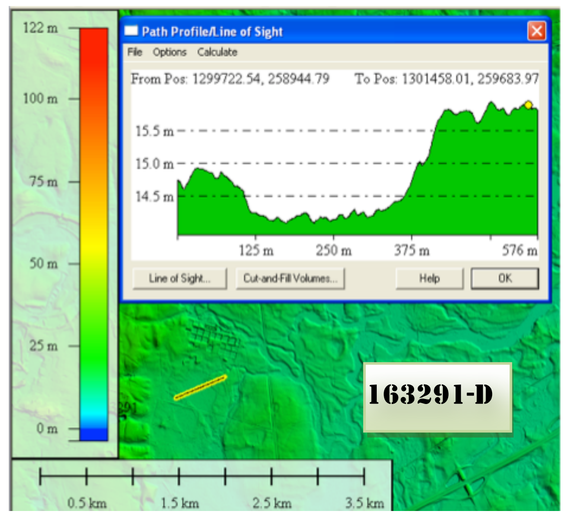
122 m
100 m
75 m
50 m
25 m
0 m
Path Profile/Line of Sight
File Options Calculate
From Pos: 1299722.54, 258944.79 To Pos: 1301458.01, 259683.97
15.5 m
15.0 m
14.5 m
125 m 250 m 375 m 576 m
Line of Sight... Cut-and-Fill Volumes... Help OK
163291-D
0.5 km 1.5 km 2.5 km 3.5 km

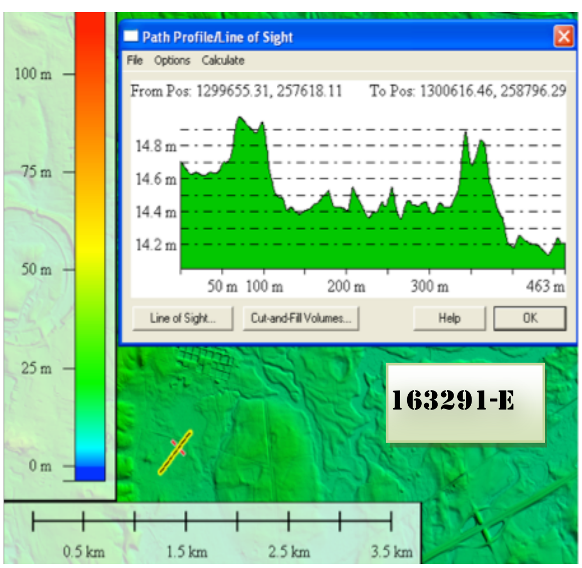
100 m
75 m
50 m
25 m
0 m
Path Profile/Line of Sight
File Options Calculate
From Pos: 1299655.31, 257618.11 To Pos: 1300616.46, 258796.29
14.8 m
14.6 m
14.4 m
14.2 m
50 m 100 m 200 m 300 m 463 m
Line of Sight... Cut-and-Fill Volumes... Help OK
163291-E
0.5 km 1.5 km 2.5 km 3.5 km

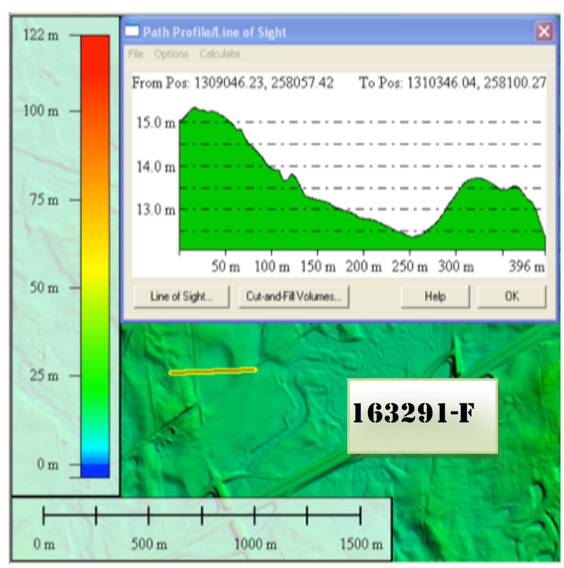
122 m
100 m
75 m
50 m
25 m
0 m
Path Profile/Line of Sight
File Options Calculate
From Pos: 1309046.23, 258057.42 To Pos: 1310346.04, 258100.27
15.0 m
14.0 m
13.0 m
50 m 100 m 150 m 200 m 250 m 300 m 396 m
Line of Sight... Cut-and-Fill Volumes... Help OK
163291-F
0 m 500 m 1000 m 1500 m

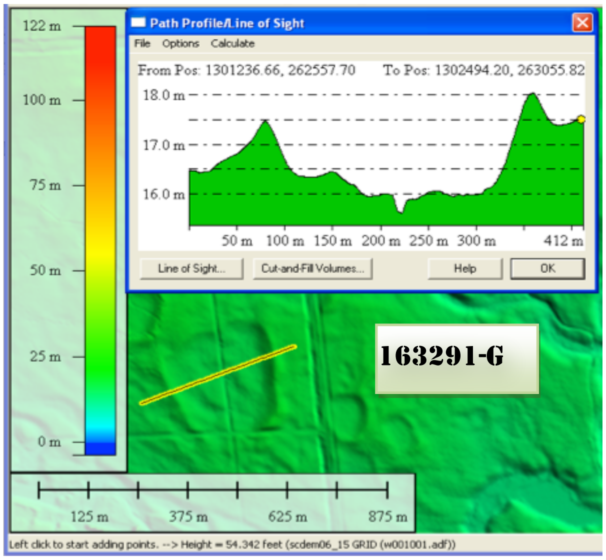
122 m
100 m
75 m
50 m
25 m
0 m
Path Profile/Line of Sight
File Options Calculate
From Pos: 1301236.66, 262557.70 To Pos: 1302494.20, 263055.82
18.0 m
17.0 m
16.0 m
50 m 100 m 150 m 200 m 250 m 300 m 412 m
Line of Sight... Cut-and-Fill Volumes... Help OK
163291-G
125 m 375 m 625 m 875 m

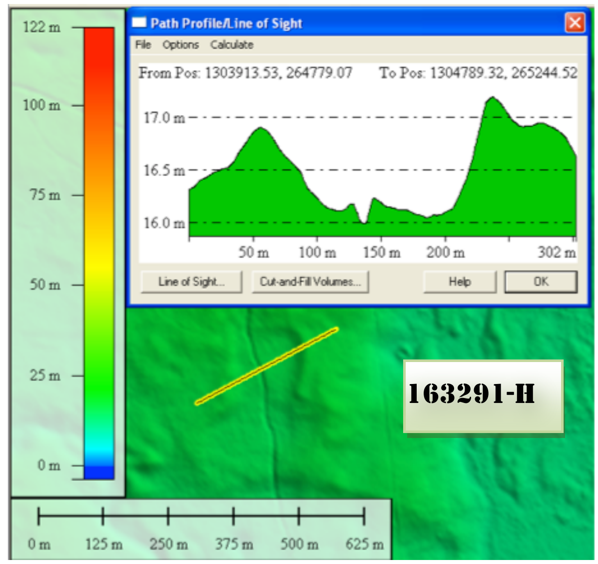
122 m
100 m
75 m
50 m
25 m
0 m
Path Profile/Line of Sight
File Options Calculate
From Pos: 1303913.53, 264779.07 To Pos: 1304789.32, 265244.52
17.0 m
16.5 m
16.0 m
50 m 100 m 150 m 200 m 302 m
Line of Sight... Cut-and-Fill Volumes... Help OK
163291-H
0 m 125 m 250 m 375 m 500 m 625 m

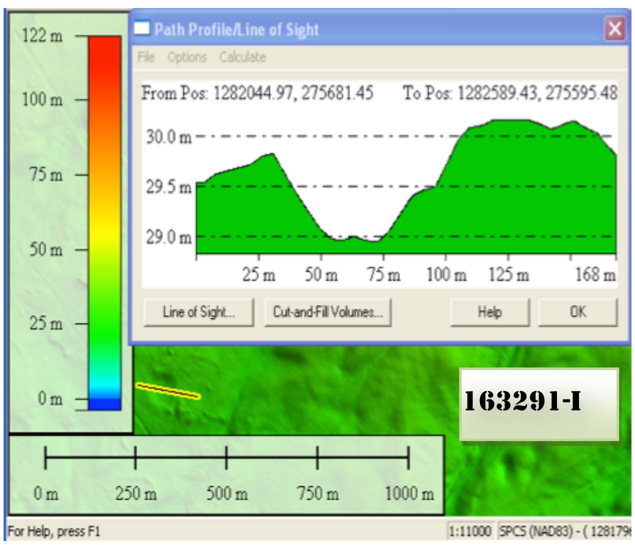
122 m
100 m
75 m
50 m
25 m
0 m
Path Profile/Line of Sight
File Options Calculate
From Pos: 1282044.97, 275681.45 To Pos: 1282589.43, 275595.48
30.0 m
29.5 m
29.0 m
25 m 50 m 75 m 100 m 125 m 168 m
Line of Sight... Cut-and-Fill Volumes... Help OK
163291-I
0 m 250 m 500 m 750 m 1000 m
For Help, press F1
1:11000 SPCS (NAD83)

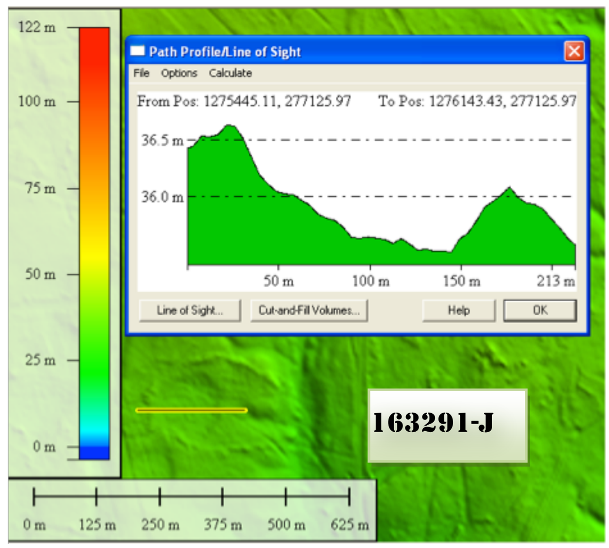
122 m
100 m
75 m
50 m
25 m
0 m
Path Profile/Line of Sight
File Options Calculate
From Pos: 1275445.11, 277125.97 To Pos: 1276143.43, 277125.97
36.5 m
36.0 m
50 m 100 m 150 m 213 m
Line of Sight... Cut-and-Fill Volumes... Help OK
163291-J
0 m 125 m 250 m 375 m 500 m 625 m

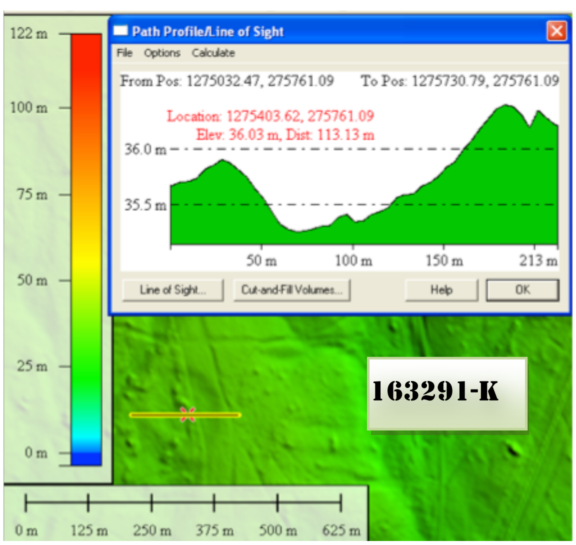
122 m
100 m
75 m
50 m
25 m
0 m
Path Profile/Line of Sight
File Options Calculate
From Pos: 1275032.47, 275761.09 To Pos: 1275730.79, 275761.09
Location: 1275403.62, 275761.09
Elev: 36.03 m, Dist: 113.13 m
36.0 m
35.5 m
50 m 100 m 150 m 213 m
Line of Sight... Cut-and-Fill Volumes... Help OK
163291-K
0 m 125 m 250 m 375 m 500 m 625 m

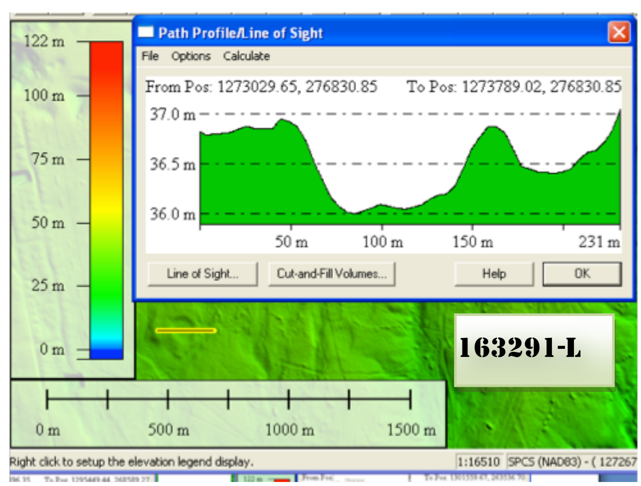
122 m
100 m
75 m
50 m
25 m
0 m
Path Profile/Line of Sight
File Options Calculate
From Pos: 1273029.65, 276830.85 To Pos: 1273789.02, 276830.85
37.0 m
36.5 m
36.0 m
50 m 100 m 150 m 231 m
Line of Sight... Cut-and-Fill Volumes... Help OK
163291-L
0 m 500 m 1000 m 1500 m
Right click to setup the elevation legend display.
1:16510 SPCS (NAD83)

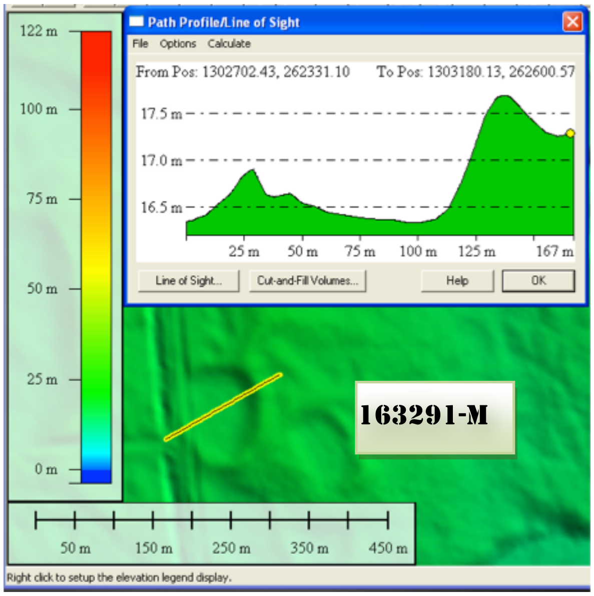
Path Profile/Line of Sight
File Options Calculate
From Pos: 1302702.43, 262331.10 To Pos: 1303180.13, 262600.57
17.5 m
17.0 m
16.5 m
25 m 50 m 75 m 100 m 125 m 167 m
Line of Sight... Cut-and-Fill Volumes... Help OK
122 m 100 m 75 m 50 m 25 m 0 m
50 m 150 m 250 m 350 m 450 m
163291-M
Right click to setup the elevation legend display.

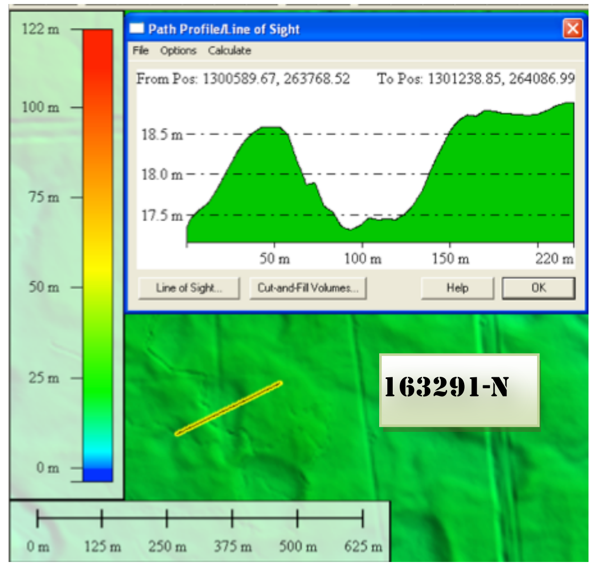
Path Profile/Line of Sight
File Options Calculate
From Pos: 1300589.67, 263768.52 To Pos: 1301238.85, 264086.99
18.5 m
18.0 m
17.5 m
50 m 100 m 150 m 220 m
Line of Sight... Cut-and-Fill Volumes... Help OK
122 m 100 m 75 m 50 m 25 m 0 m
0 m 125 m 250 m 375 m 500 m 625 m
163291-N

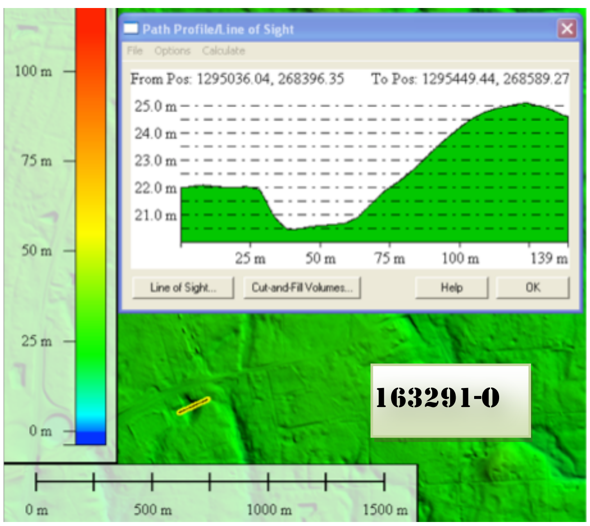
Path Profile/Line of Sight
File Options Calculate
From Pos: 1295036.04, 268396.35 To Pos: 1295449.44, 268589.27
25.0 m
24.0 m
23.0 m
22.0 m
21.0 m
25 m 50 m 75 m 100 m 139 m
Line of Sight... Cut-and-Fill Volumes... Help OK
100 m 75 m 50 m 25 m 0 m
0 m 500 m 1000 m 1500 m
163291-O

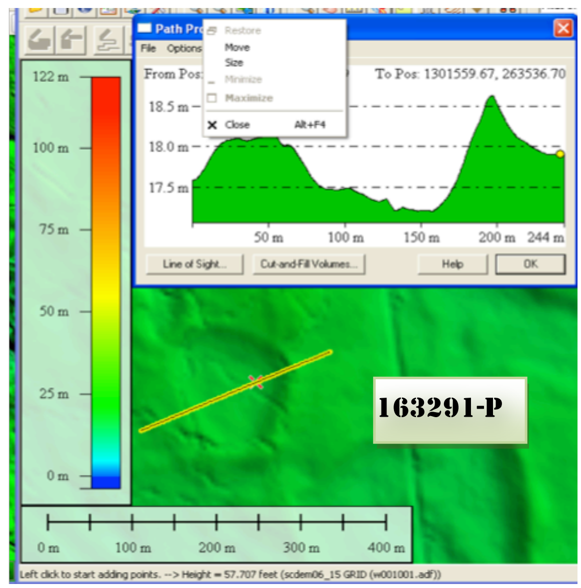
Path Pro
File Options
Restore
Move
Size
Minimize
Maximize
Close Alt+F4
From Pos: To Pos: 1301559.67, 263536.70
18.5 m
18.0 m
17.5 m
50 m 100 m 150 m 200 m 244 m
Line of Sight... Cut-and-Fill Volumes... Help OK
122 m 100 m 75 m 50 m 25 m 0 m
0 m 100 m 200 m 300 m 400 m
163291-P
Left click to start adding points. --> Height = 57.707 feet (scdem06_15 GRID (w001001.adf))

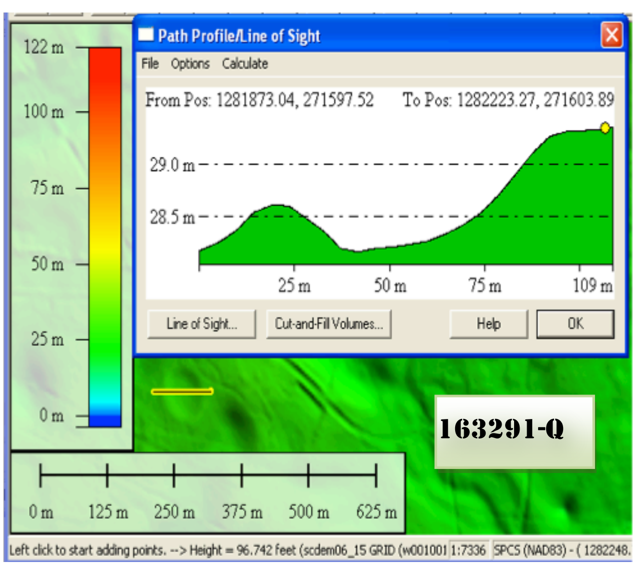
Path Profile/Line of Sight
File Options Calculate
From Pos: 1281873.04, 271597.52 To Pos: 1282223.27, 271603.89
29.0 m
28.5 m
25 m 50 m 75 m 109 m
Line of Sight... Cut-and-Fill Volumes... Help OK
122 m 100 m 75 m 50 m 25 m 0 m
0 m 125 m 250 m 375 m 500 m 625 m
163291-Q
Left click to start adding points. --> Height = 96.742 feet (scdem06_15 GRID (w001001 1:7336 SPCS (NAD83) - (1282248.

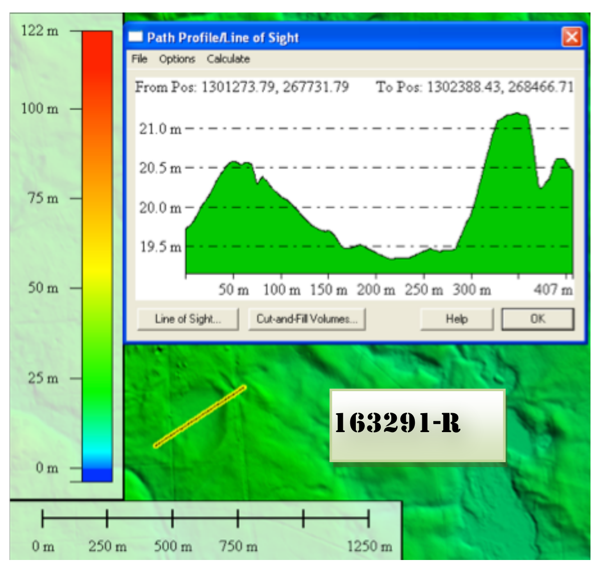
Path Profile/Line of Sight
File Options Calculate
From Pos: 1301273.79, 267731.79 To Pos: 1302388.43, 268466.71
21.0 m
20.5 m
20.0 m
19.5 m
50 m 100 m 150 m 200 m 250 m 300 m 407 m
Line of Sight... Cut-and-Fill Volumes... Help OK
122 m 100 m 75 m 50 m 25 m 0 m
0 m 250 m 500 m 750 m 1250 m
163291-R

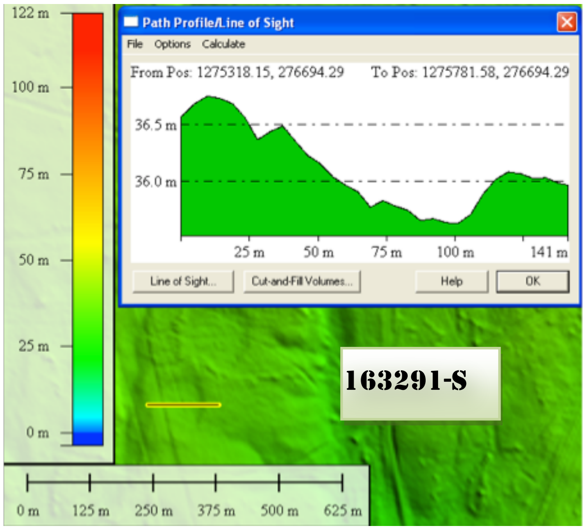
Path Profile/Line of Sight
File Options Calculate
From Pos: 1275318.15, 276694.29 To Pos: 1275781.58, 276694.29
36.5 m
36.0 m
25 m 50 m 75 m 100 m 141 m
Line of Sight... Cut-and-Fill Volumes... Help OK
122 m
100 m
75 m
50 m
25 m
0 m
0 m 125 m 250 m 375 m 500 m 625 m
163291-S

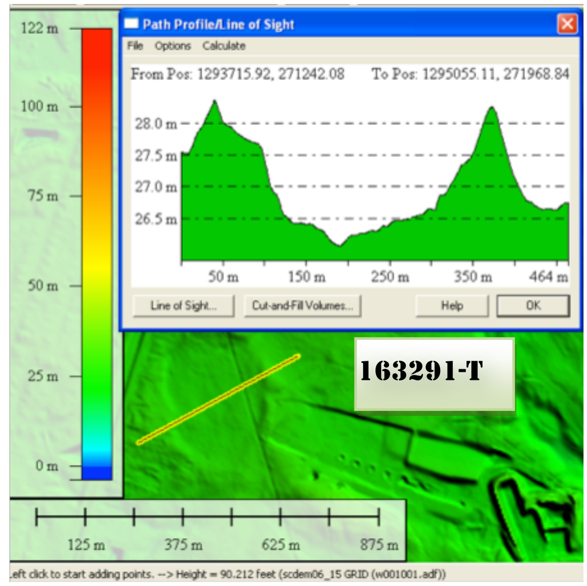
Path Profile/Line of Sight
File Options Calculate
From Pos: 1293715.92, 271242.08 To Pos: 1295055.11, 271968.84
28.0 m
27.5 m
27.0 m
26.5 m
50 m 150 m 250 m 350 m 464 m
Line of Sight... Cut-and-Fill Volumes... Help OK
122 m
100 m
75 m
50 m
25 m
0 m
125 m 375 m 625 m 875 m
163291-T
Left click to start adding points. --> Height = 90.212 feet (scdem06_15 GRID (w001001.adf))

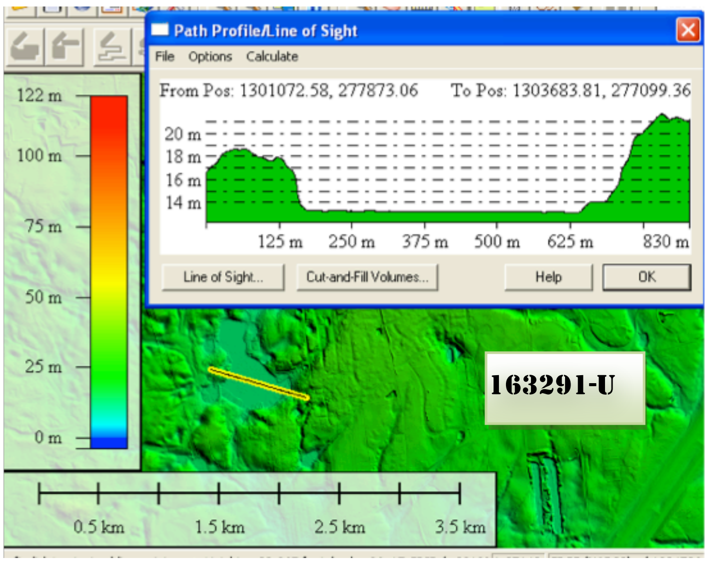
Path Profile/Line of Sight
File Options Calculate
From Pos: 1301072.58, 277873.06 To Pos: 1303683.81, 277099.36
20 m
18 m
16 m
14 m
125 m 250 m 375 m 500 m 625 m 830 m
Line of Sight... Cut-and-Fill Volumes... Help OK
122 m
100 m
75 m
50 m
25 m
0 m
0.5 km 1.5 km 2.5 km 3.5 km
163291-U

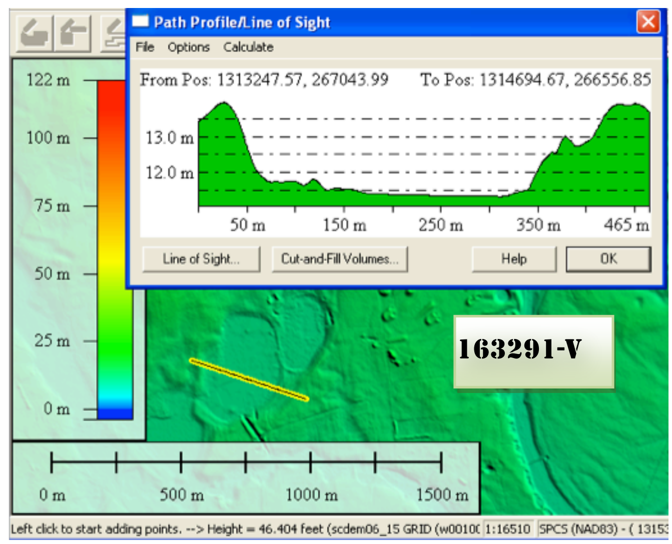
Path Profile/Line of Sight
File Options Calculate
From Pos: 1313247.57, 267043.99 To Pos: 1314694.67, 266556.85
13.0 m
12.0 m
50 m 150 m 250 m 350 m 465 m
Line of Sight... Cut-and-Fill Volumes... Help OK
122 m
100 m
75 m
50 m
25 m
0 m
0 m 500 m 1000 m 1500 m
163291-V
Left click to start adding points. --> Height = 46.404 feet (scdem06_15 GRID (w00100 1:16510 SPCS (NAD83) - (13153

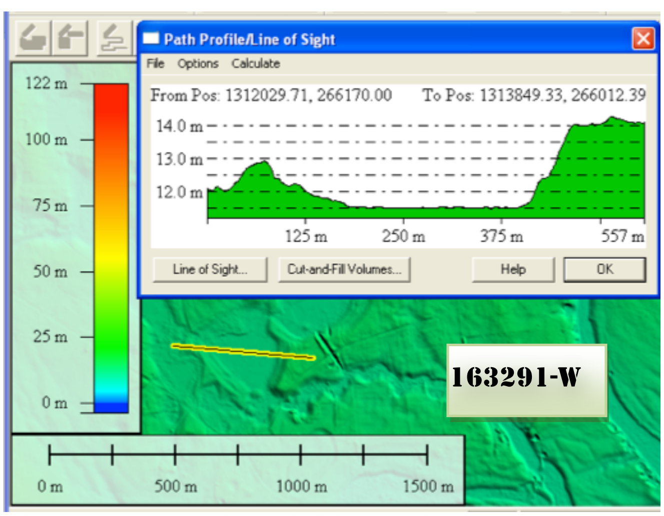
Path Profile/Line of Sight
File Options Calculate
From Pos: 1312029.71, 266170.00 To Pos: 1313849.33, 266012.39
14.0 m
13.0 m
12.0 m
125 m 250 m 375 m 557 m
Line of Sight... Cut-and-Fill Volumes... Help OK
122 m
100 m
75 m
50 m
25 m
0 m
0 m 500 m 1000 m 1500 m
163291-W

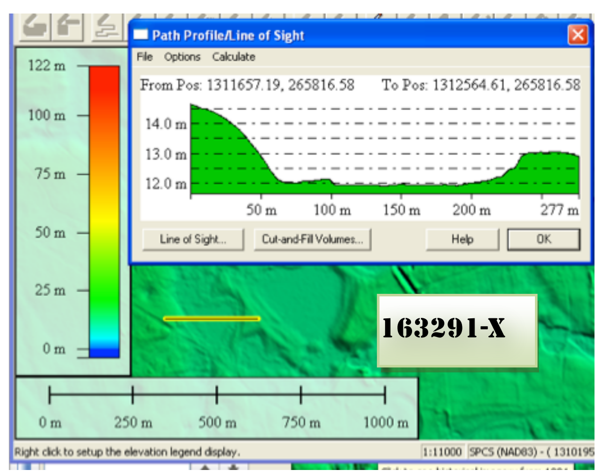
Path Profile/Line of Sight
File Options Calculate
From Pos: 1311657.19, 265816.58 To Pos: 1312564.61, 265816.58
14.0 m
13.0 m
12.0 m
50 m 100 m 150 m 200 m 277 m
Line of Sight... Cut-and-Fill Volumes... Help OK
122 m
100 m
75 m
50 m
25 m
0 m
0 m 250 m 500 m 750 m 1000 m
163291-X
Right click to setup the elevation legend display. 1:11000 SPCS (NAD83) - (1310195

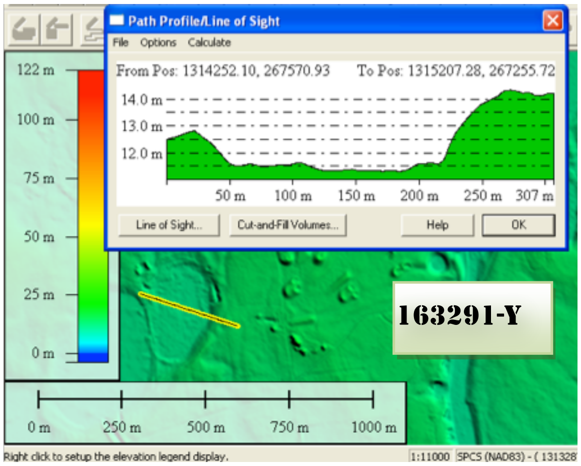
Path Profile/Line of Sight
File Options Calculate
From Pos: 1314252.10, 267570.93 To Pos: 1315207.28, 267255.72
14.0 m
13.0 m
12.0 m
50 m 100 m 150 m 200 m 250 m 307 m
Line of Sight... Cut-and-Fill Volumes... Help OK
122 m 100 m 75 m 50 m 25 m 0 m
163291-Y
0 m 250 m 500 m 750 m 1000 m
Right click to setup the elevation legend display.
1:11000 SPCS (NAD83)

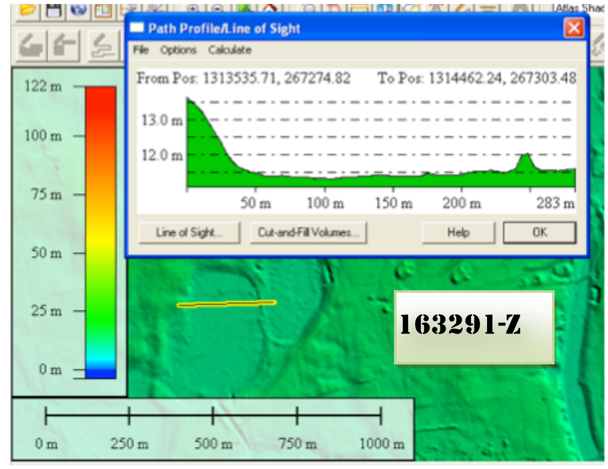
Path Profile/Line of Sight
File Options Calculate
From Pos: 1313535.71, 267274.82 To Pos: 1314462.24, 267303.48
13.0 m
12.0 m
50 m 100 m 150 m 200 m 283 m
Line of Sight... Cut-and-Fill Volumes... Help OK
122 m 100 m 75 m 50 m 25 m 0 m
163291-Z
0 m 250 m 500 m 750 m 1000 m

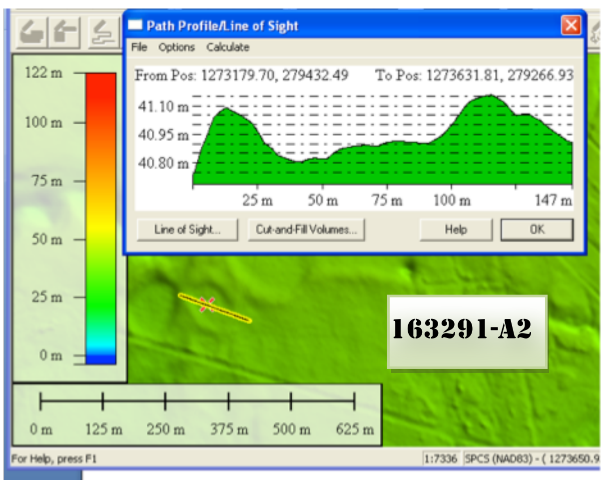
Path Profile/Line of Sight
File Options Calculate
From Pos: 1273179.70, 279432.49 To Pos: 1273631.81, 279266.93
41.10 m
40.95 m
40.80 m
25 m 50 m 75 m 100 m 147 m
Line of Sight... Cut-and-Fill Volumes... Help OK
122 m 100 m 75 m 50 m 25 m 0 m
163291-A2
0 m 125 m 250 m 375 m 500 m 625 m
For Help, press F1
1:7336 SPCS (NAD83)

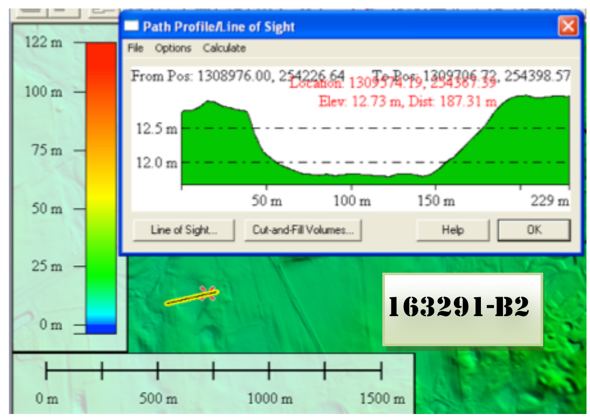
Path Profile/Line of Sight
File Options Calculate
From Pos: 1308976.00, 254226.64 To Pos: 1309706.72, 254398.57
Elev: 12.73 m, Dist: 187.31 m
12.5 m
12.0 m
50 m 100 m 150 m 229 m
Line of Sight... Cut-and-Fill Volumes... Help OK
122 m 100 m 75 m 50 m 25 m 0 m
163291-B2
0 m 500 m 1000 m 1500 m

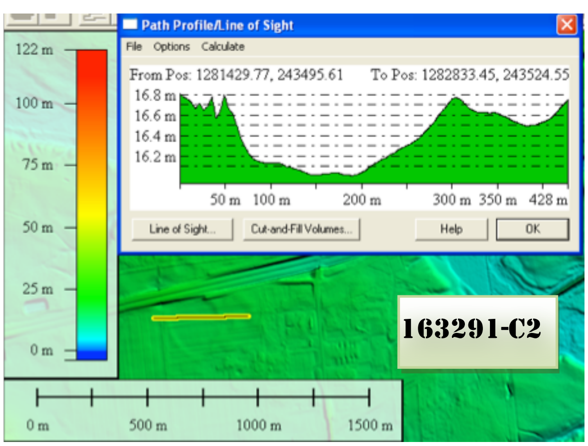
Path Profile/Line of Sight
File Options Calculate
From Pos: 1281429.77, 243495.61 To Pos: 1282833.45, 243524.55
16.8 m
16.6 m
16.4 m
16.2 m
50 m 100 m 200 m 300 m 350 m 428 m
Line of Sight... Cut-and-Fill Volumes... Help OK
122 m 100 m 75 m 50 m 25 m 0 m
163291-C2
0 m 500 m 1000 m 1500 m

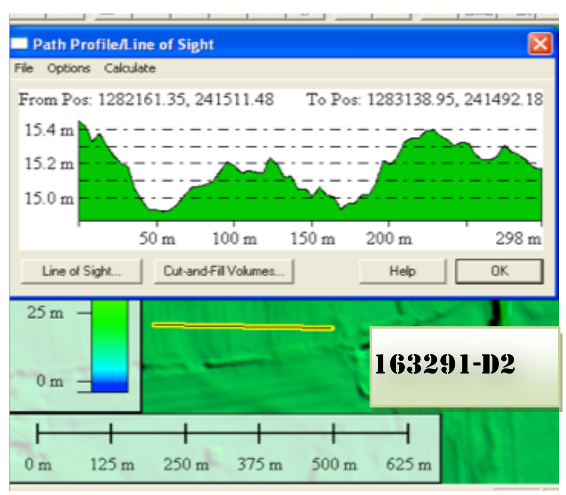
Path Profile/Line of Sight
File Options Calculate
From Pos: 1282161.35, 241511.48 To Pos: 1283138.95, 241492.18
15.4 m
15.2 m
15.0 m
50 m 100 m 150 m 200 m 298 m
Line of Sight... Cut-and-Fill Volumes... Help OK
25 m 0 m
163291-D2
0 m 125 m 250 m 375 m 500 m 625 m

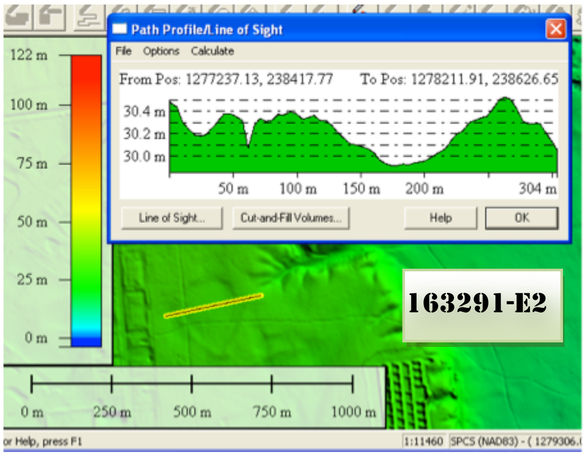
Path Profile/Line of Sight
File Options Calculate
From Pos: 1277237.13, 238417.77 To Pos: 1278211.91, 238626.65
30.4 m
30.2 m
30.0 m
50 m 100 m 150 m 200 m 304 m
Line of Sight... Cut-and-Fill Volumes... Help OK
122 m 100 m 75 m 50 m 25 m 0 m
0 m 250 m 500 m 750 m 1000 m
163291-E2
For Help, press F1
1:11460 SPCS (NAD83)

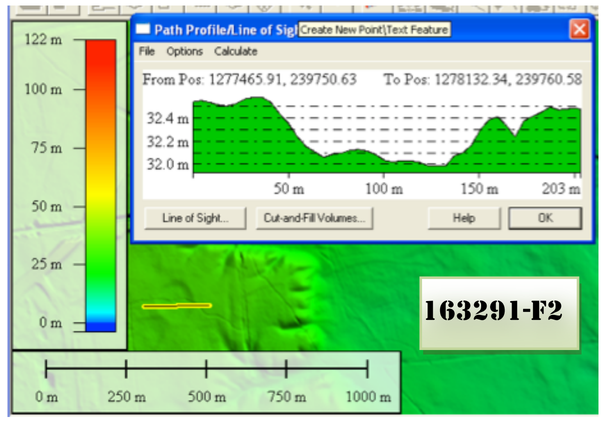
Path Profile/Line of Sight
Create New Point\Text Feature
File Options Calculate
From Pos: 1277465.91, 239750.63 To Pos: 1278132.34, 239760.58
32.4 m
32.2 m
32.0 m
50 m 100 m 150 m 203 m
Line of Sight... Cut-and-Fill Volumes... Help OK
122 m 100 m 75 m 50 m 25 m 0 m
0 m 250 m 500 m 750 m 1000 m
163291-F2

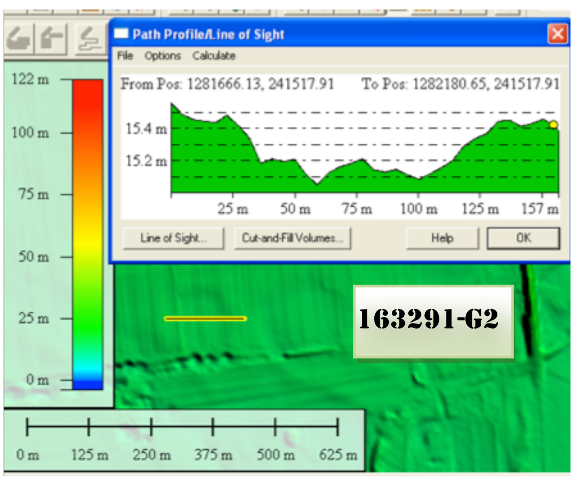
Path Profile/Line of Sight
File Options Calculate
From Pos: 1281666.13, 241517.91 To Pos: 1282180.65, 241517.91
15.4 m
15.2 m
25 m 50 m 75 m 100 m 125 m 157 m
Line of Sight... Cut-and-Fill Volumes... Help OK
122 m 100 m 75 m 50 m 25 m 0 m
0 m 125 m 250 m 375 m 500 m 625 m
163291-G2

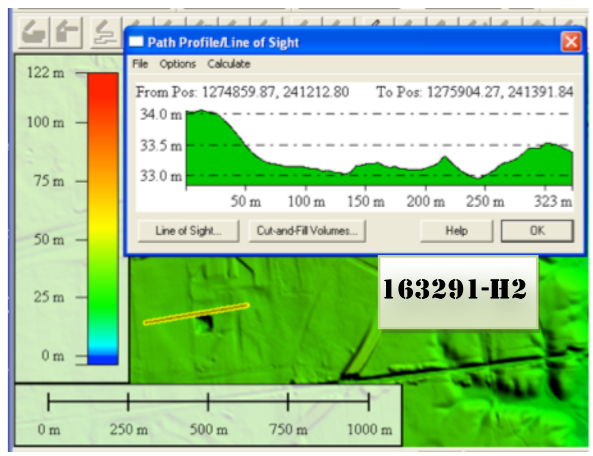
Path Profile/Line of Sight
File Options Calculate
From Pos: 1274859.87, 241212.80 To Pos: 1275904.27, 241391.84
34.0 m
33.5 m
33.0 m
50 m 100 m 150 m 200 m 250 m 323 m
Line of Sight... Cut-and-Fill Volumes... Help OK
122 m 100 m 75 m 50 m 25 m 0 m
0 m 250 m 500 m 750 m 1000 m
163291-H2

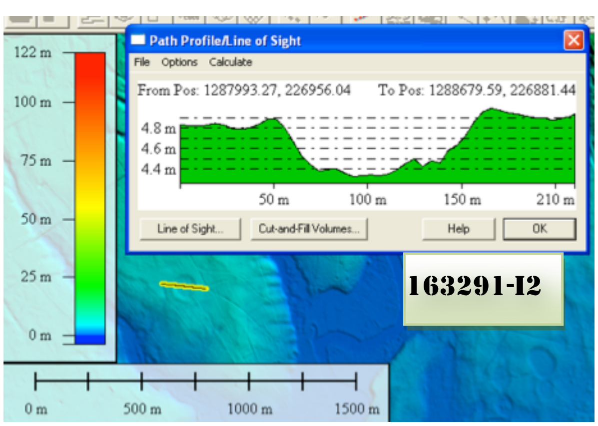
Path Profile/Line of Sight
File Options Calculate
From Pos: 1287993.27, 226956.04 To Pos: 1288679.59, 226881.44
4.8 m
4.6 m
4.4 m
50 m 100 m 150 m 210 m
Line of Sight... Cut-and-Fill Volumes... Help OK
122 m 100 m 75 m 50 m 25 m 0 m
0 m 500 m 1000 m 1500 m
163291-I2

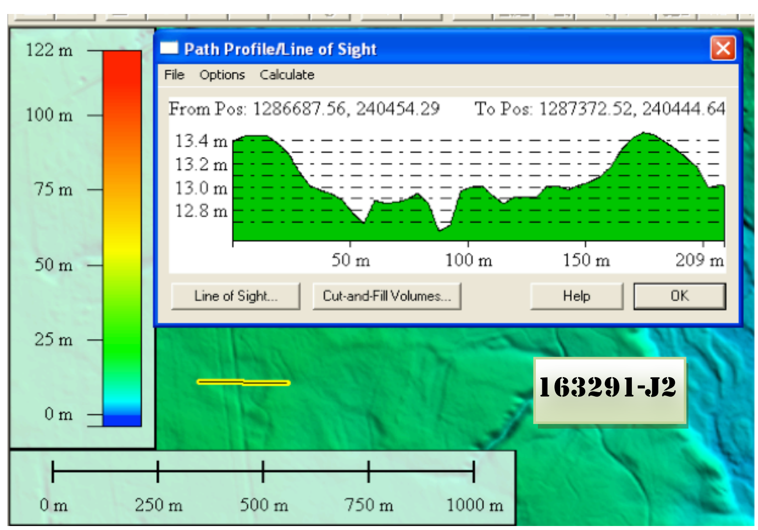
Path Profile/Line of Sight
File Options Calculate
From Pos: 1286687.56, 240454.29 To Pos: 1287372.52, 240444.64
13.4 m
13.2 m
13.0 m
12.8 m
50 m 100 m 150 m 209 m
Line of Sight... Cut-and-Fill Volumes... Help OK
122 m 100 m 75 m 50 m 25 m 0 m
0 m 250 m 500 m 750 m 1000 m
163291-J2

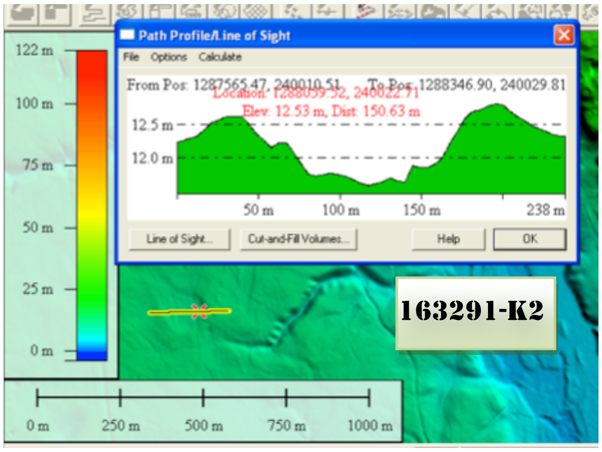
Path Profile/Line of Sight
File Options Calculate
From Pos: 1287565.47, 240010.51 To Pos: 1288346.90, 240029.81
Elev: 12.53 m, Dist: 150.63 m
12.5 m
12.0 m
50 m 100 m 150 m 238 m
Line of Sight... Cut-and-Fill Volumes... Help OK
122 m 100 m 75 m 50 m 25 m 0 m
0 m 250 m 500 m 750 m 1000 m
163291-K2

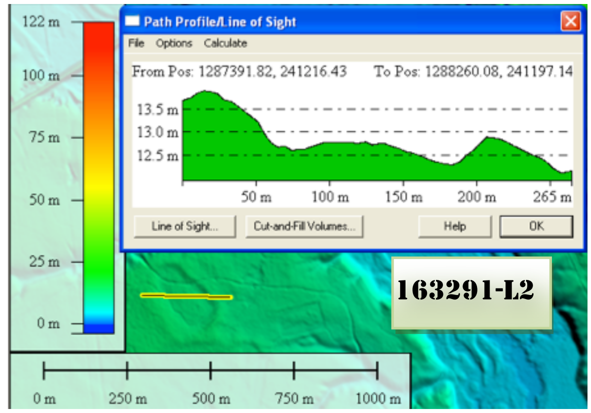
Path Profile/Line of Sight
File Options Calculate
From Pos: 1287391.82, 241216.43 To Pos: 1288260.08, 241197.14
13.5 m
13.0 m
12.5 m
50 m 100 m 150 m 200 m 265 m
Line of Sight... Cut-and-Fill Volumes... Help OK
122 m 100 m 75 m 50 m 25 m 0 m
0 m 250 m 500 m 750 m 1000 m
163291-L2

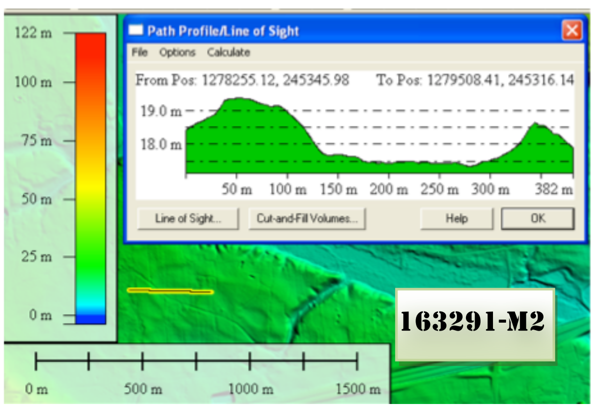
Path Profile/Line of Sight
File Options Calculate
From Pos: 1278255.12, 245345.98 To Pos: 1279508.41, 245316.14
19.0 m
18.0 m
50 m 100 m 150 m 200 m 250 m 300 m 382 m
Line of Sight... Cut-and-Fill Volumes... Help OK
122 m 100 m 75 m 50 m 25 m 0 m
0 m 500 m 1000 m 1500 m
163291-M2

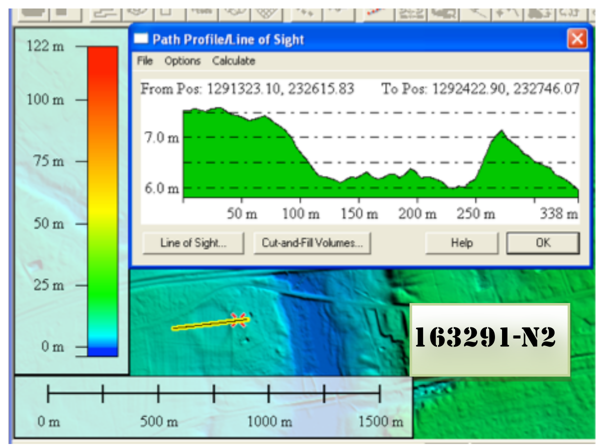
Path Profile/Line of Sight
File Options Calculate
From Pos: 1291323.10, 232615.83 To Pos: 1292422.90, 232746.07
7.0 m
6.0 m
50 m 100 m 150 m 200 m 250 m 338 m
Line of Sight... Cut-and-Fill Volumes... Help OK
122 m 100 m 75 m 50 m 25 m 0 m
0 m 500 m 1000 m 1500 m
163291-N2

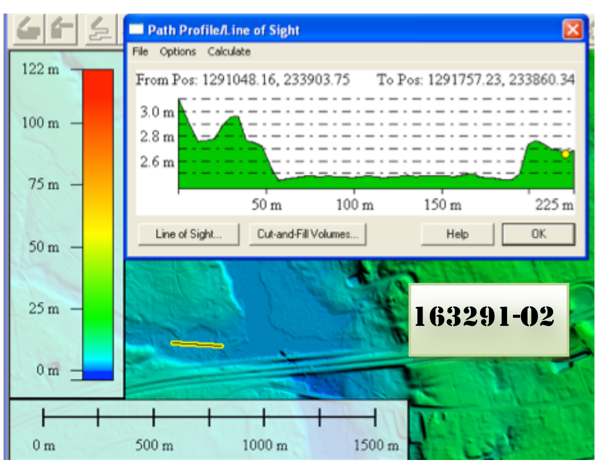
Path Profile/Line of Sight
File Options Calculate
From Pos: 1291048.16, 233903.75 To Pos: 1291757.23, 233860.34
3.0 m
2.8 m
2.6 m
50 m 100 m 150 m 225 m
Line of Sight... Cut-and-Fill Volumes... Help OK
122 m 100 m 75 m 50 m 25 m 0 m
0 m 500 m 1000 m 1500 m
163291-O2

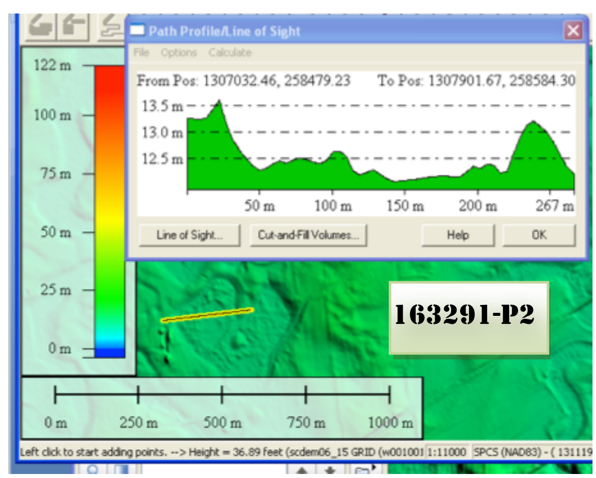
Path Profile/Line of Sight
File Options Calculate
From Pos: 1307032.46, 258479.23 To Pos: 1307901.67, 258584.30
13.5 m
13.0 m
12.5 m
50 m 100 m 150 m 200 m 267 m
Line of Sight... Cut-and-Fill Volumes... Help OK
122 m 100 m 75 m 50 m 25 m 0 m
0 m 250 m 500 m 750 m 1000 m
163291-P2

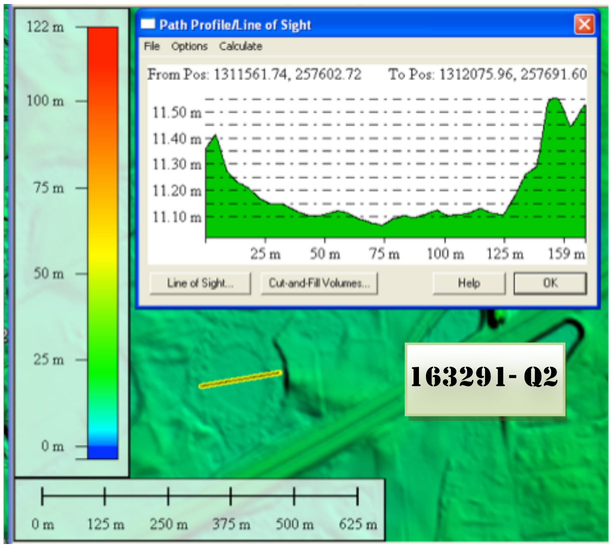
Path Profile/Line of Sight
File Options Calculate
From Pos: 1311561.74, 257602.72 To Pos: 1312075.96, 257691.60
11.50 m
11.40 m
11.30 m
11.20 m
11.10 m
25 m 50 m 75 m 100 m 125 m 159 m
Line of Sight... Cut-and-Fill Volumes... Help OK
122 m 100 m 75 m 50 m 25 m 0 m
0 m 125 m 250 m 375 m 500 m 625 m
163291- Q2

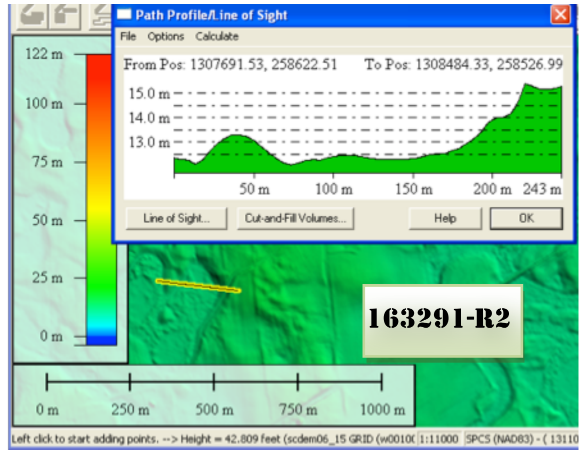
Path Profile/Line of Sight
File Options Calculate
From Pos: 1307691.53, 258622.51 To Pos: 1308484.33, 258526.99
15.0 m
14.0 m
13.0 m
50 m 100 m 150 m 200 m 243 m
Line of Sight... Cut-and-Fill Volumes... Help OK
122 m 100 m 75 m 50 m 25 m 0 m
0 m 250 m 500 m 750 m 1000 m
163291-R2

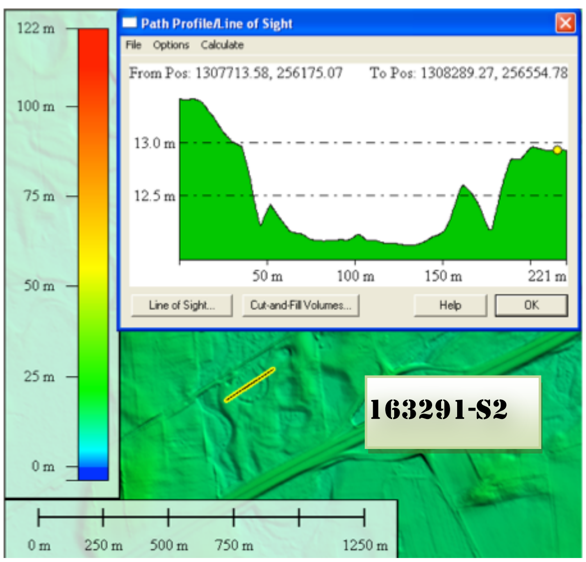
Path Profile/Line of Sight
File Options Calculate
From Pos: 1307713.58, 256175.07 To Pos: 1308289.27, 256554.78
13.0 m
12.5 m
50 m 100 m 150 m 221 m
Line of Sight... Cut-and-Fill Volumes... Help OK
122 m 100 m 75 m 50 m 25 m 0 m
0 m 250 m 500 m 750 m 1250 m
163291-S2

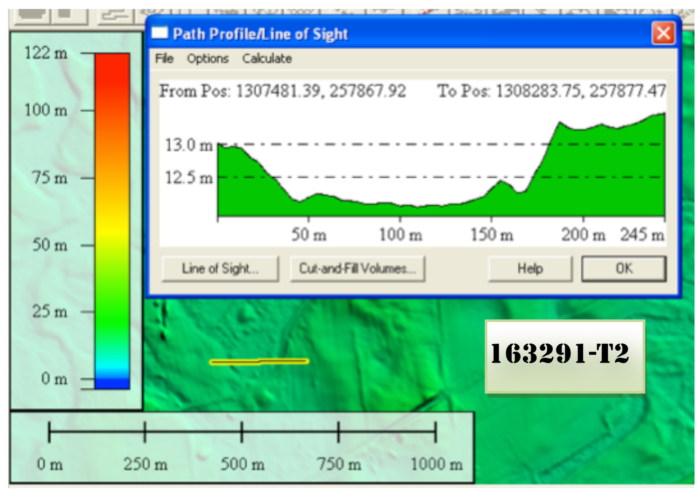
Path Profile/Line of Sight
File Options Calculate
From Pos: 1307481.39, 257867.92 To Pos: 1308283.75, 257877.47
13.0 m
12.5 m
50 m 100 m 150 m 200 m 245 m
Line of Sight... Cut-and-Fill Volumes... Help OK
122 m 100 m 75 m 50 m 25 m 0 m
0 m 250 m 500 m 750 m 1000 m
163291-T2

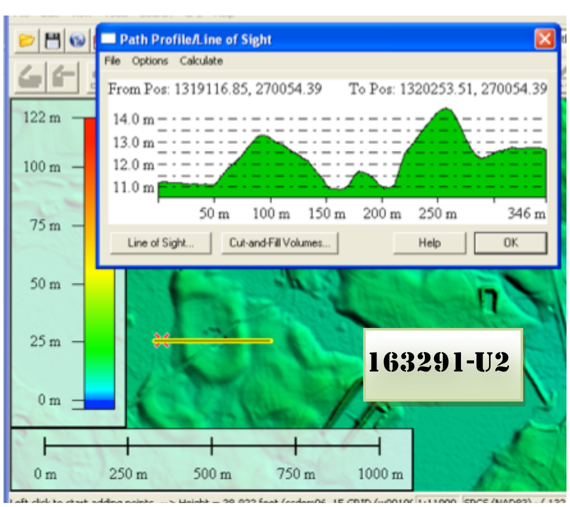
Path Profile/Line of Sight
File Options Calculate
From Pos: 1319116.85, 270054.39 To Pos: 1320253.51, 270054.39
14.0 m
13.0 m
12.0 m
11.0 m
50 m 100 m 150 m 200 m 250 m 346 m
Line of Sight... Cut-and-Fill Volumes... Help OK
122 m 100 m 75 m 50 m 25 m 0 m
0 m 250 m 500 m 750 m 1000 m
163291-U2

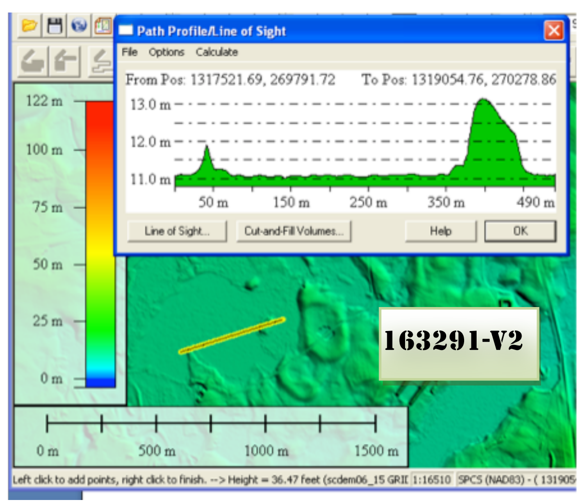
Path Profile/Line of Sight
File Options Calculate
From Pos: 1317521.69, 269791.72 To Pos: 1319054.76, 270278.86
13.0 m
12.0 m
11.0 m
50 m 150 m 250 m 350 m 490 m
Line of Sight... Cut-and-Fill Volumes... Help OK
122 m 100 m 75 m 50 m 25 m 0 m
0 m 500 m 1000 m 1500 m
163291-V2

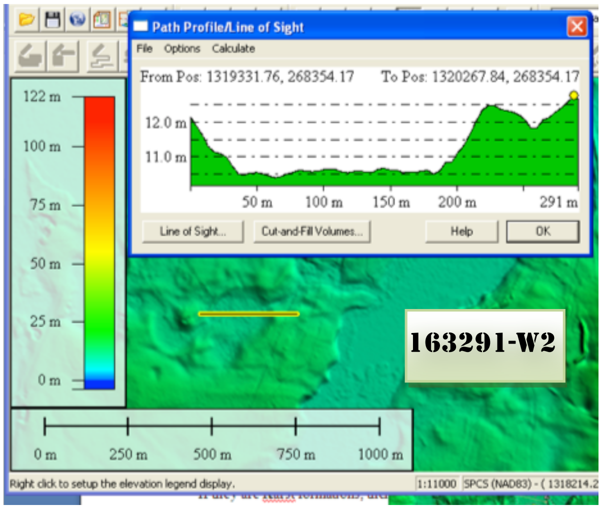
Path Profile/Line of Sight
File Options Calculate
From Pos: 1319331.76, 268354.17
To Pos: 1320267.84, 268354.17
12.0 m
11.0 m
50 m 100 m 150 m 200 m 291 m
Line of Sight... Cut-and-Fill Volumes... Help OK
122 m 100 m 75 m 50 m 25 m 0 m
0 m 250 m 500 m 750 m 1000 m
163291-W2
Right click to setup the elevation legend display.
1:11000 SPCS (NAD83)

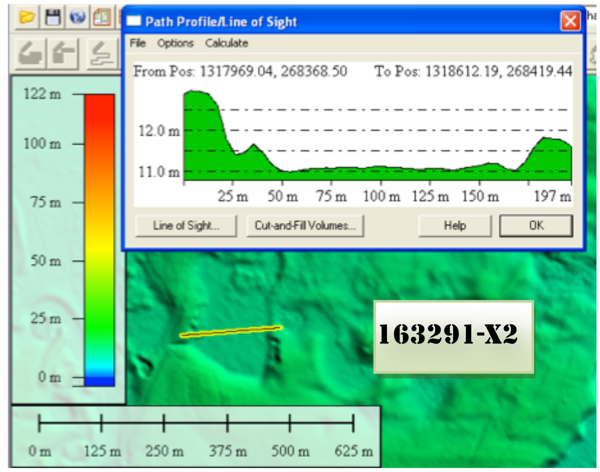
Path Profile/Line of Sight
File Options Calculate
From Pos: 1317969.04, 268368.50
To Pos: 1318612.19, 268419.44
12.0 m
11.0 m
25 m 50 m 75 m 100 m 125 m 150 m 197 m
Line of Sight... Cut-and-Fill Volumes... Help OK
122 m 100 m 75 m 50 m 25 m 0 m
0 m 125 m 250 m 375 m 500 m 625 m
163291-X2

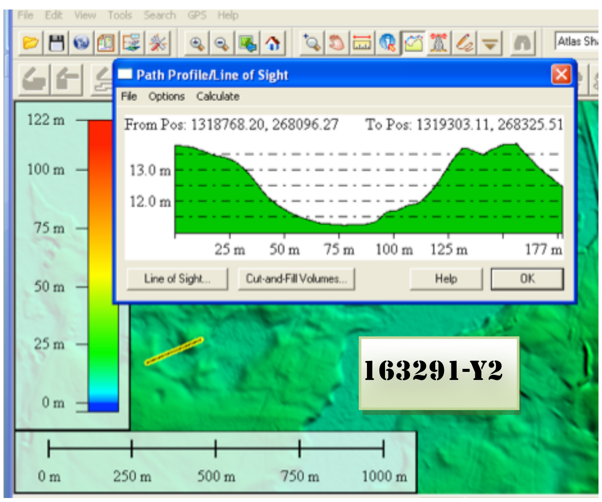
File Edit View Tools Search GPS Help
Path Profile/Line of Sight
File Options Calculate
From Pos: 1318768.20, 268096.27
To Pos: 1319303.11, 268325.51
13.0 m
12.0 m
25 m 50 m 75 m 100 m 125 m 177 m
Line of Sight... Cut-and-Fill Volumes... Help OK
122 m 100 m 75 m 50 m 25 m 0 m
0 m 250 m 500 m 750 m 1000 m
163291-Y2

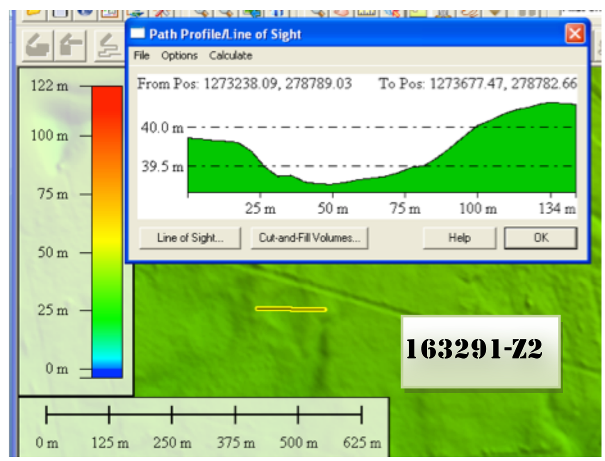
Path Profile/Line of Sight
File Options Calculate
From Pos: 1273238.09, 278789.03
To Pos: 1273677.47, 278782.66
40.0 m
39.5 m
25 m 50 m 75 m 100 m 134 m
Line of Sight... Cut-and-Fill Volumes... Help OK
122 m 100 m 75 m 50 m 25 m 0 m
0 m 125 m 250 m 375 m 500 m 625 m
163291-Z2

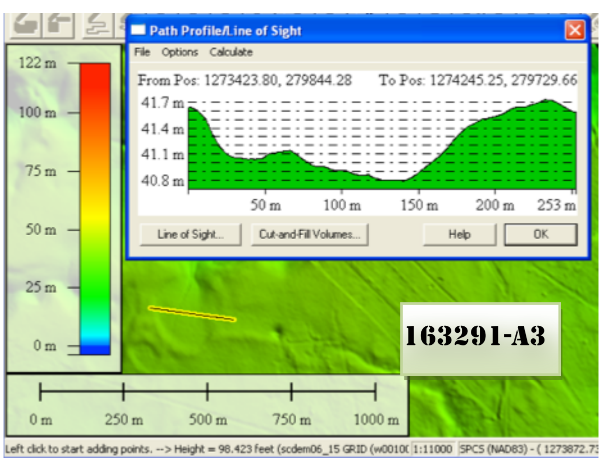
Path Profile/Line of Sight
File Options Calculate
From Pos: 1273423.80, 279844.28
To Pos: 1274245.25, 279729.66
41.7 m
41.4 m
41.1 m
40.8 m
50 m 100 m 150 m 200 m 253 m
Line of Sight... Cut-and-Fill Volumes... Help OK
122 m 100 m 75 m 50 m 25 m 0 m
0 m 250 m 500 m 750 m 1000 m
163291-A3
Left click to start adding points. --> Height = 98.423 feet (scdem06_15 GRID
1:11000 SPCS (NAD83)

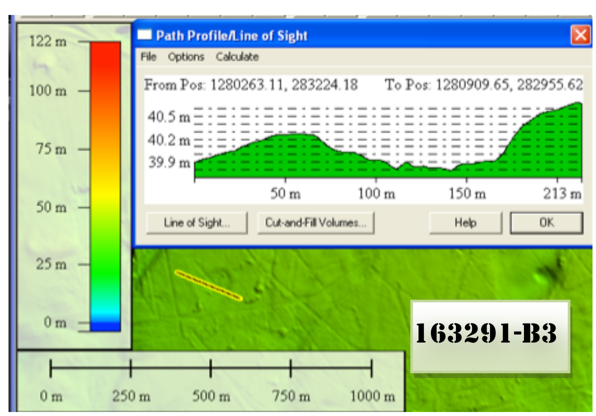
Path Profile/Line of Sight
File Options Calculate
From Pos: 1280263.11, 283224.18
To Pos: 1280909.65, 282955.62
40.5 m
40.2 m
39.9 m
50 m 100 m 150 m 213 m
Line of Sight... Cut-and-Fill Volumes... Help OK
122 m 100 m 75 m 50 m 25 m 0 m
0 m 250 m 500 m 750 m 1000 m
163291-B3

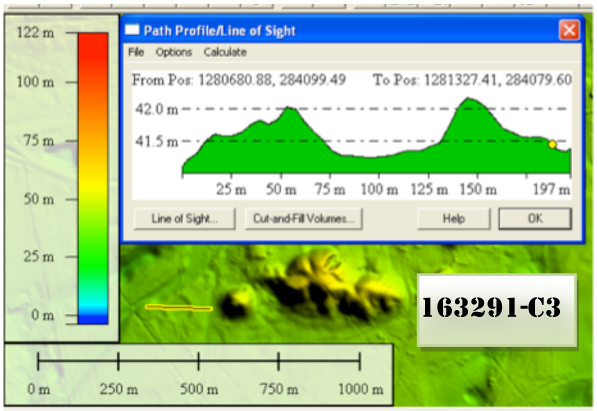
Path Profile/Line of Sight
File Options Calculate
From Pos: 1280680.88, 284099.49 To Pos: 1281327.41, 284079.60
42.0 m
41.5 m
25 m 50 m 75 m 100 m 125 m 150 m 197 m
Line of Sight... Cut-and-Fill Volumes... Help OK
122 m 100 m 75 m 50 m 25 m 0 m
0 m 250 m 500 m 750 m 1000 m
163291-C3

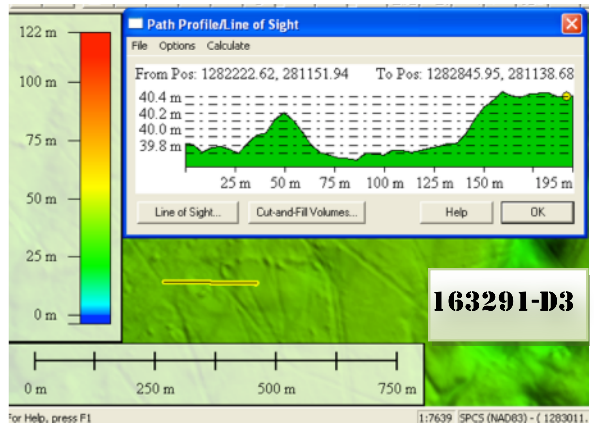
Path Profile/Line of Sight
File Options Calculate
From Pos: 1282222.62, 281151.94 To Pos: 1282845.95, 281138.68
40.4 m
40.2 m
40.0 m
39.8 m
25 m 50 m 75 m 100 m 125 m 150 m 195 m
Line of Sight... Cut-and-Fill Volumes... Help OK
122 m 100 m 75 m 50 m 25 m 0 m
0 m 250 m 500 m 750 m
163291-D3
For Help, press F1
1:7639 SPCS (NAD83) - (1283011.

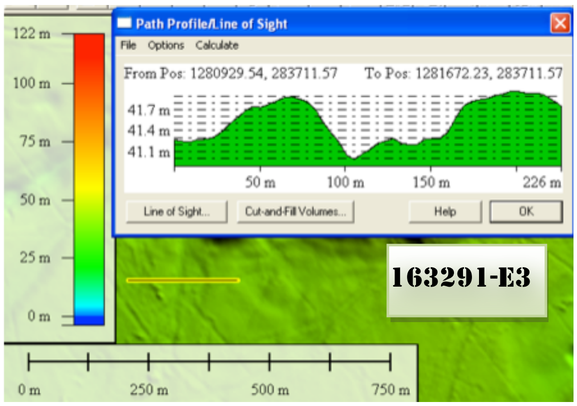
Path Profile/Line of Sight
File Options Calculate
From Pos: 1280929.54, 283711.57 To Pos: 1281672.23, 283711.57
41.7 m
41.4 m
41.1 m
50 m 100 m 150 m 226 m
Line of Sight... Cut-and-Fill Volumes... Help OK
122 m 100 m 75 m 50 m 25 m 0 m
0 m 250 m 500 m 750 m
163291-E3

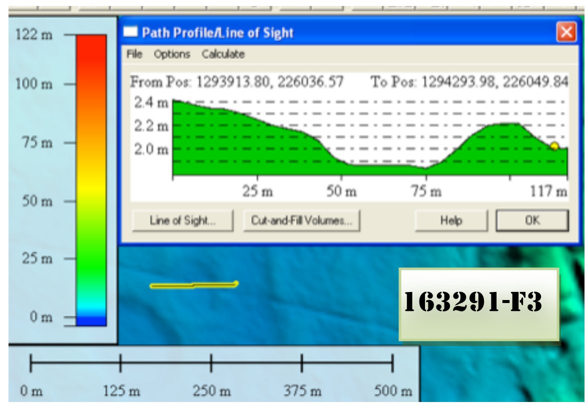
Path Profile/Line of Sight
File Options Calculate
From Pos: 1293913.80, 226036.57 To Pos: 1294293.98, 226049.84
2.4 m
2.2 m
2.0 m
25 m 50 m 75 m 117 m
Line of Sight... Cut-and-Fill Volumes... Help OK
122 m 100 m 75 m 50 m 25 m 0 m
0 m 125 m 250 m 375 m 500 m
163291-F3

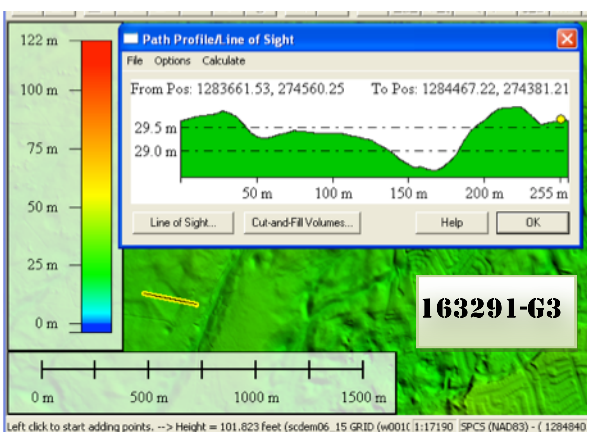
Path Profile/Line of Sight
File Options Calculate
From Pos: 1283661.53, 274560.25 To Pos: 1284467.22, 274381.21
29.5 m
29.0 m
50 m 100 m 150 m 200 m 255 m
Line of Sight... Cut-and-Fill Volumes... Help OK
122 m 100 m 75 m 50 m 25 m 0 m
0 m 500 m 1000 m 1500 m
163291-G3
Left click to start adding points. --> Height = 101.823 feet (scdem06_15 GRID (w001(1:17190 SPCS (NAD83) - (1284840

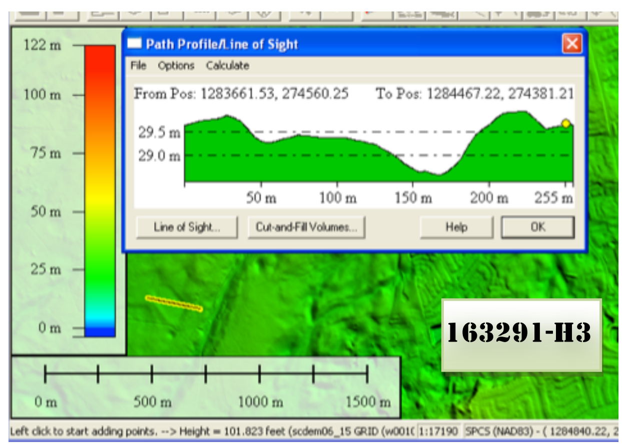
Path Profile/Line of Sight
File Options Calculate
From Pos: 1283661.53, 274560.25 To Pos: 1284467.22, 274381.21
29.5 m
29.0 m
50 m 100 m 150 m 200 m 255 m
Line of Sight... Cut-and-Fill Volumes... Help OK
122 m 100 m 75 m 50 m 25 m 0 m
0 m 500 m 1000 m 1500 m
163291-H3
Left click to start adding points. --> Height = 101.823 feet (scdem06_15 GRID (w001(1:17190 SPCS (NAD83) - (1284840.22, 2

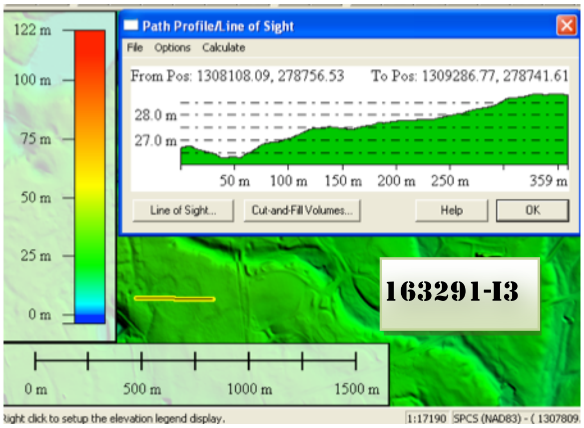
Path Profile/Line of Sight
From Pos: 1308108.09, 278756.53
To Pos: 1309286.77, 278741.61
28.0 m
27.0 m
50 m 100 m 150 m 200 m 250 m 359 m
Line of Sight...
Cut-and-Fill Volumes...
Help
OK
163291-I3
122 m 100 m 75 m 50 m 25 m 0 m
0 m 500 m 1000 m 1500 m
Right click to setup the elevation legend display.

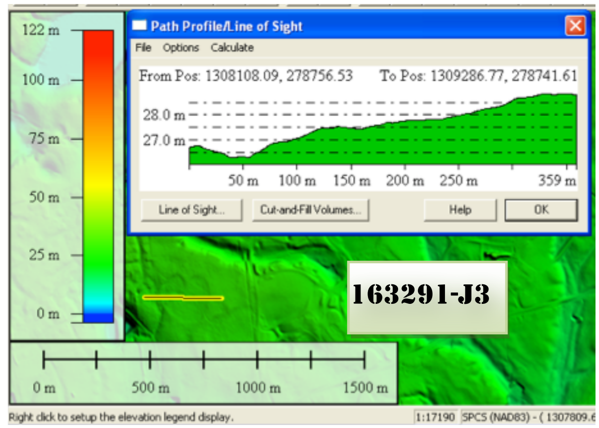
Path Profile/Line of Sight
From Pos: 1308108.09, 278756.53
To Pos: 1309286.77, 278741.61
28.0 m
27.0 m
50 m 100 m 150 m 200 m 250 m 359 m
Line of Sight...
Cut-and-Fill Volumes...
Help
OK
163291-J3
122 m 100 m 75 m 50 m 25 m 0 m
0 m 500 m 1000 m 1500 m
Right click to setup the elevation legend display.

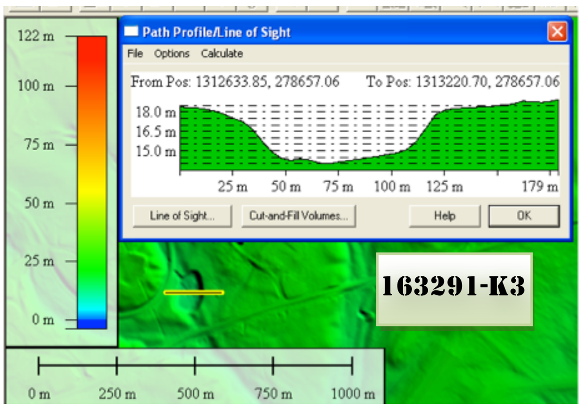
Path Profile/Line of Sight
From Pos: 1312633.85, 278657.06
To Pos: 1313220.70, 278657.06
18.0 m
16.5 m
15.0 m
25 m 50 m 75 m 100 m 125 m 179 m
Line of Sight...
Cut-and-Fill Volumes...
Help
OK
163291-K3
122 m 100 m 75 m 50 m 25 m 0 m
0 m 250 m 500 m 750 m 1000 m

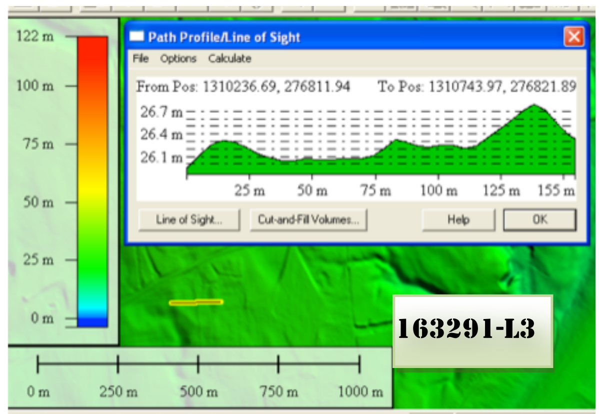
Path Profile/Line of Sight
From Pos: 1310236.69, 276811.94
To Pos: 1310743.97, 276821.89
26.7 m
26.4 m
26.1 m
25 m 50 m 75 m 100 m 125 m 155 m
Line of Sight...
Cut-and-Fill Volumes...
Help
OK
163291-L3
122 m 100 m 75 m 50 m 25 m 0 m
0 m 250 m 500 m 750 m 1000 m

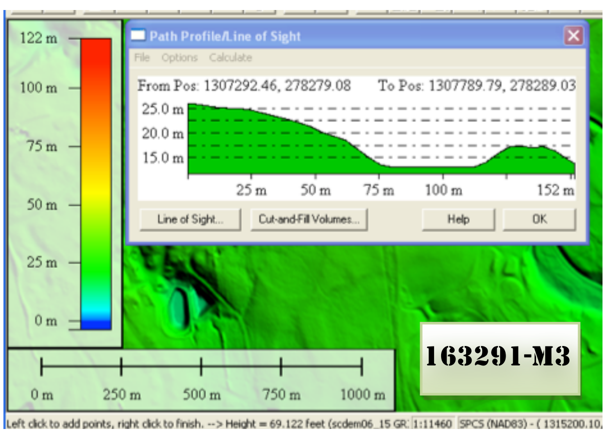
Path Profile/Line of Sight
From Pos: 1307292.46, 278279.08
To Pos: 1307789.79, 278289.03
25.0 m
20.0 m
15.0 m
25 m 50 m 75 m 100 m 152 m
Line of Sight...
Cut-and-Fill Volumes...
Help
OK
163291-M3
122 m 100 m 75 m 50 m 25 m 0 m
0 m 250 m 500 m 750 m 1000 m

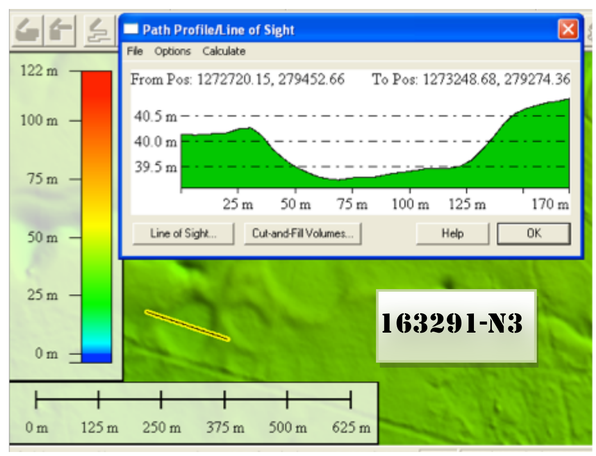
Path Profile/Line of Sight
From Pos: 1272720.15, 279452.66
To Pos: 1273248.68, 279274.36
40.5 m
40.0 m
39.5 m
25 m 50 m 75 m 100 m 125 m 170 m
Line of Sight...
Cut-and-Fill Volumes...
Help
OK
163291-N3
122 m 100 m 75 m 50 m 25 m 0 m
0 m 125 m 250 m 375 m 500 m 625 m

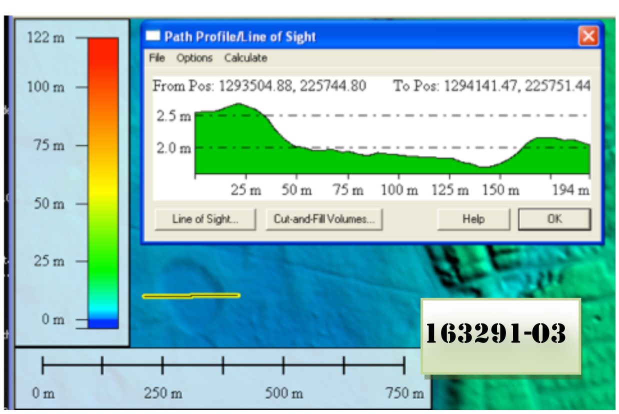
Path Profile/Line of Sight
From Pos: 1293504.88, 225744.80
To Pos: 1294141.47, 225751.44
2.5 m
2.0 m
25 m 50 m 75 m 100 m 125 m 150 m 194 m
Line of Sight...
Cut-and-Fill Volumes...
Help
OK
163291-O3
122 m 100 m 75 m 50 m 25 m 0 m
0 m 250 m 500 m 750 m

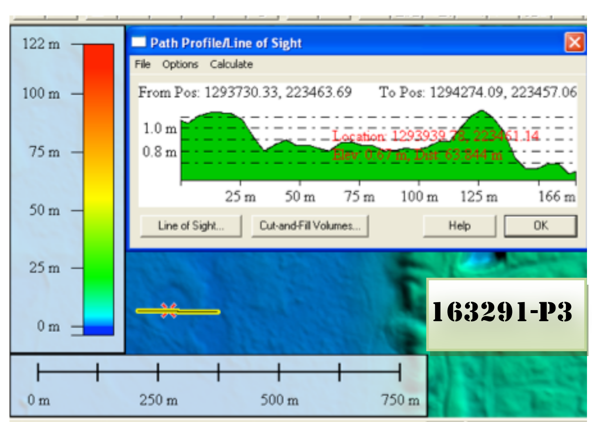
Path Profile/Line of Sight
From Pos: 1293730.33, 223463.69
To Pos: 1294274.09, 223457.06
1.0 m
0.8 m
25 m 50 m 75 m 100 m 125 m 166 m
Line of Sight...
Cut-and-Fill Volumes...
Help
OK
163291-P3
122 m 100 m 75 m 50 m 25 m 0 m
0 m 250 m 500 m 750 m

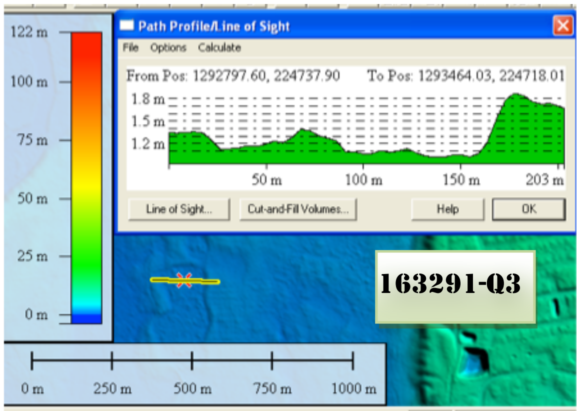

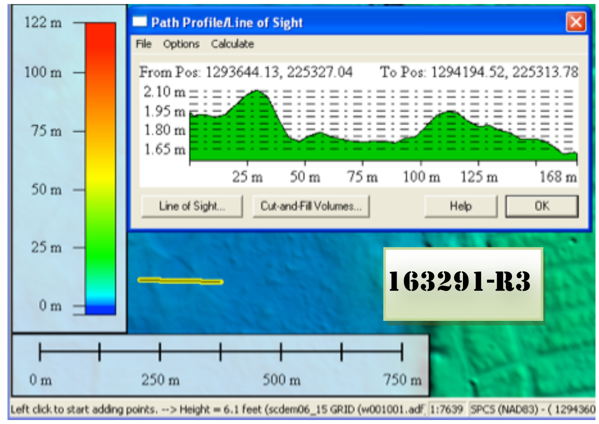

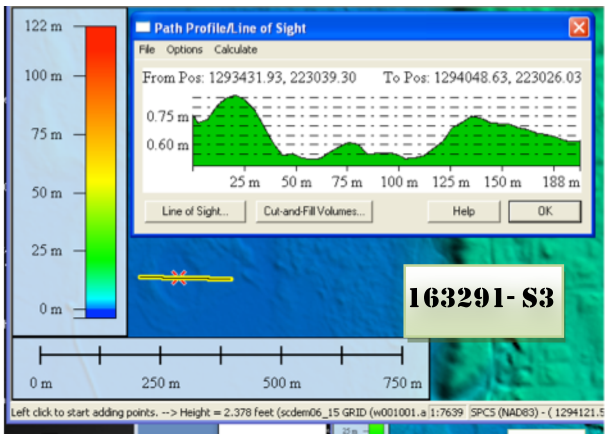

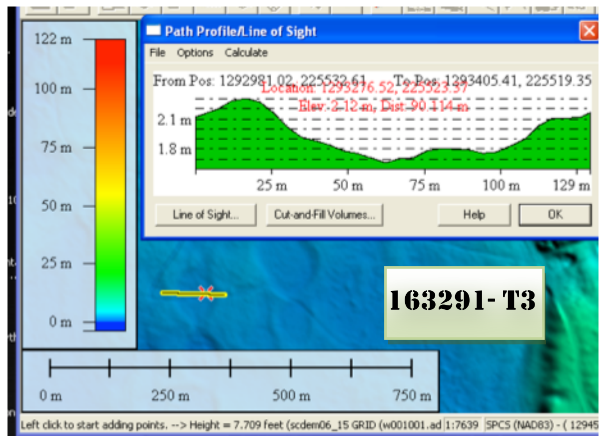

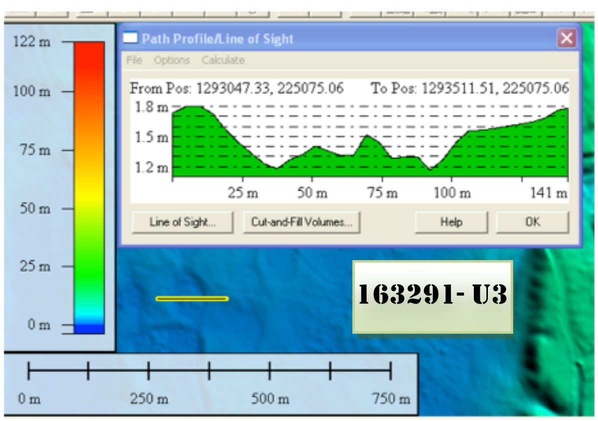

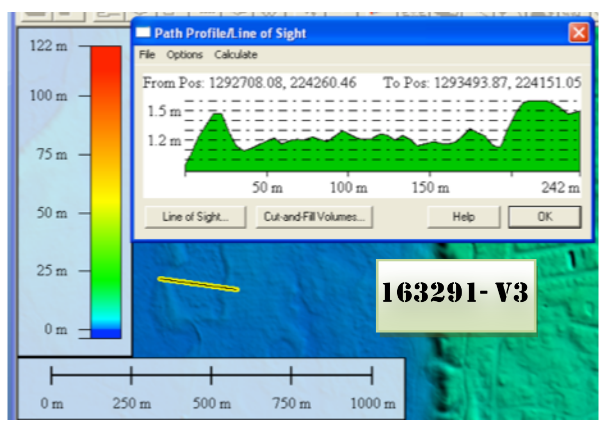

Discussion

Documenting bay formations on Long Island is a significant step in understanding these enigmatic land features. Although the results do not yield insight into the formation of the shallow rimmed depressions, their presence on Long Island imposes a time constraint on the initial basin development. Long Island did not exist before the onset of the Wisconsian glaciation. Rather Long Island was deposited during the advance and retreat of at least two glaciations approximately 20,000 years ago.

Therefore the bay formations on Long Island must be younger than 20,000 years old. In order to understand the chronological value of bays present on Long Island it is imperative to review the glacial geology that formed Long Island.

The formation of Long Island:

The surface of Long Island did not exist prior to the last glacial maximum, some 20,000 years ago. The following is a brief summary of the glacial history of Long Island, ages are in calendar years, calibrated using Calib Software (Stuiver et al., 2005). Glaciers advanced over the Long Island area several times in late Wisconsian, beginning 25,000 years ago and melted away by 20,000 years ago (Sirkin, 1982). Figure 10 depicts the Long Island Sound area 21,000 years ago during the maximum advance of the Laurentide Ice Sheet. During the Late Wisconsin the Laurentide Ice Sheet covered most of Canada, the Upper Midwest, and New England, see figure 11.

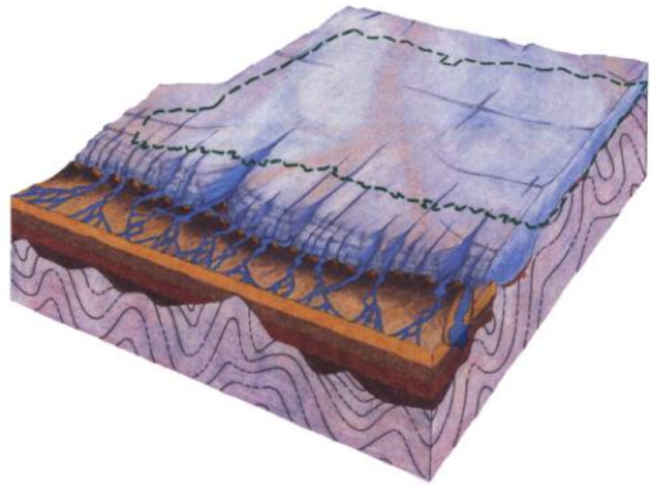

Figure 10: Diagram showing what the area of present day long island sound looked like approximately 21,000 years ago. (Lewis 2001, Needell 1987)

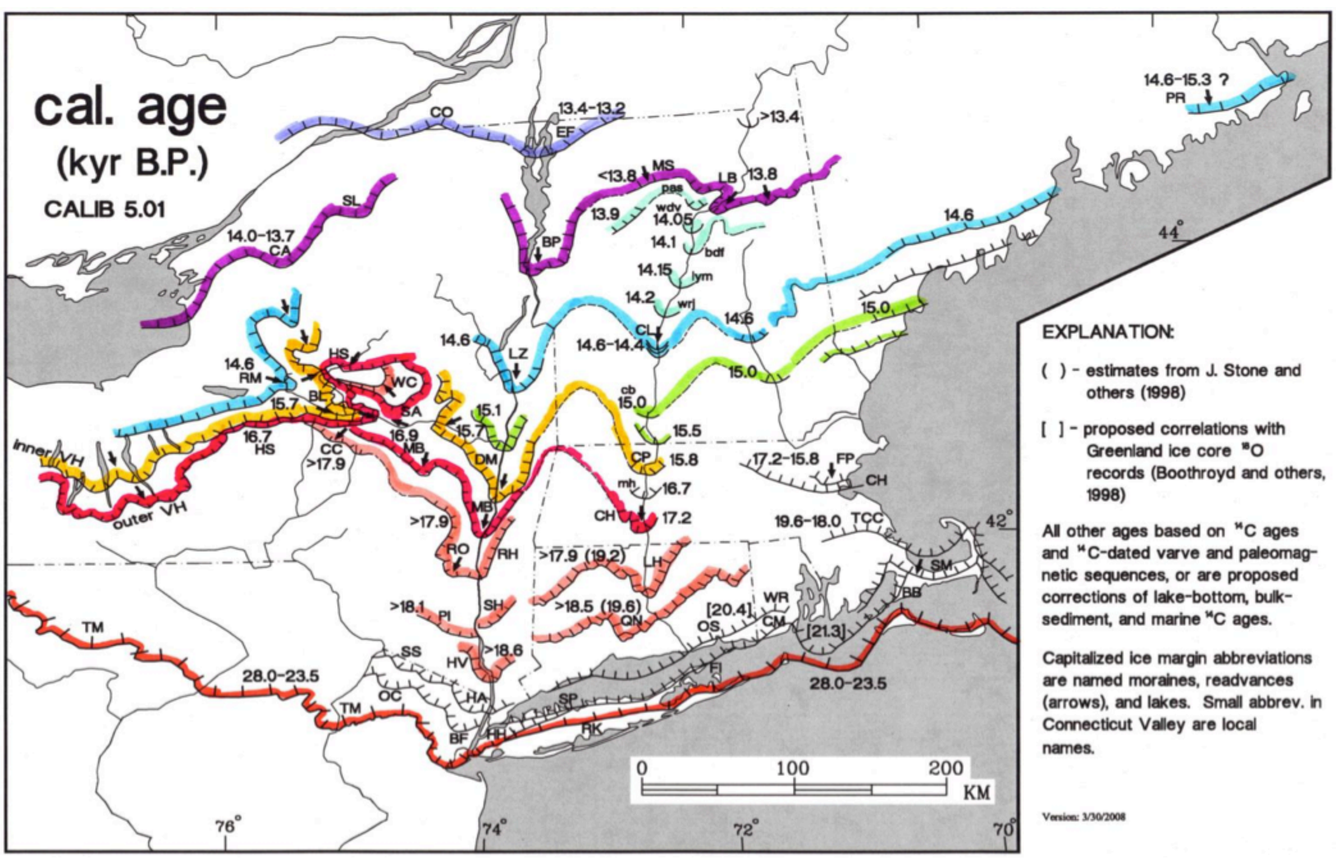

Figure 11: Map showing the position of the Laurentide Ice Sheet as it advanced and retreated across North America during the last Ice Age. (Ridge, 2011)

During this glacial maximum, sea level was about 300 feet lower than it is today. The pre-glacial topography of the region was altered but not completely changed by these ice advances (Patton, 1992). Long Island sediments and structure are the result of a minimum of two separate glacial advances during this time period (Lewis and Needell, 1987). This is evident by the presence of two moraines, the northern Harbor Hill Moraine and the southern Ronkonkoma Moraine. The outwash channels originating from the Harbor Hill Moraine intersect the Ronkonkoma Moraine. This provides evidence that the Harbor Hill Moraine is younger and a product of a second glacial advance after the initial advance and retreat that formed the Ronkonkoma Moraine (Bennington, 2003). It took about 1,500 years for the Wisconsinan glacier to melt back from its position along the north shore of Long Island to the position depicted in figure 12. Analysis of boulders from the Ronkonkoma moraine, give Cosmogenic exposure ages of ca 18,000 years (Cabe et al., 2006). This research suggests that the Harbor Hill Moraine formed only slightly after the Ronkonkoma Moraine about 20,000 years ago (Sirkin, 1982). The advance and subsequent retreat of the Laurentide ice sheet produced the elongated fish shape island south of Connecticut, known today as Long Island.

Long Islands Landscape and Scuttle Hole Ponds:

It was originally believed that the Ronkonkoma Moraine was a terminal push moraine indicating the furthest extent of the ice sheet (Fuller, 1914 and Merrill et al.,1902). However, the presence of till overlying outwash sediments southward beyond the moraine indicate the glacier advanced over the moraine after forming it (King et al, 2003 and Schmitt 2006). During periods of glacial retreat, the melt water carved out an outwash plain valleys with a braided appearance. However, when the glacier re-advanced over Long Island, these outwash plain valleys were buried by the advancing ice, till, and outwash deposits. This explains Long Island's lack of braided stream network normally characteristic of an outwash plain valley. King et al. (2003) provided evidence of presence of till south of Ronkonkoma Moraine from West Hampton to the east to North Amityville to the west. The till in this region is described by them as a surface layer often covered by loess and it is underlain by stratified sand and gravel or clay. In other words "out- wash plain valleys formed from the melting water of glacier were covered by the till and sediments left behind by the retreating glacier" (Sen-Das, 2007). The absence of outwash plain valleys in Long Island suggests that melt water from glaciers is not the agent that eroded the Dry Valleys of Long Island. In 2007, Soma Sen dedicated her graduate thesis to understanding the erosional agents leading to the development of the straight parallel dry valleys clearly visible along the south shore of Long Island. Sen concludes that the dry valleys formed while Long Island sediments were in a state of permafrost. The erosion due to heightened surface runoff over the impermeable ground caused the dentrical patterns observed today in dry valleys. The subsequent melting of the permafrost resulted in increased infiltration and a perched water table. This triggered the sapping or head ward erosion of the dry valleys. This resulted in parallel stream valleys with rectangular watersheds, steep gradients and few tributaries. As the permafrost continued to melt, the

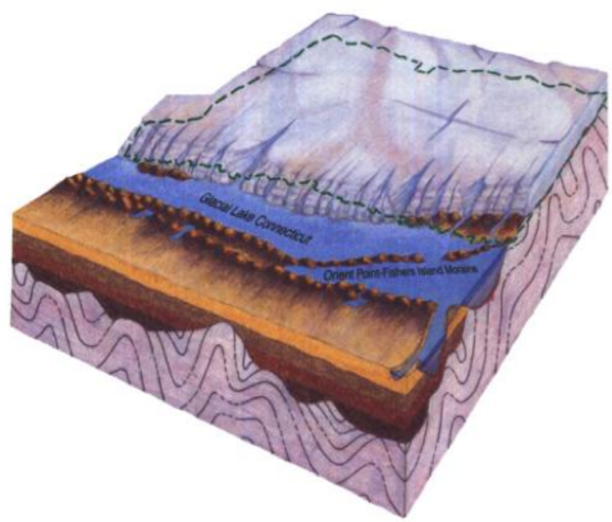

Figure 12: A view of Connecticut and the moraines on Long Island as the Laurentide Ice Sheet retreated. About 17,500 years ago.

perched water table eventually subsided leaving the northern parts of the valleys dry. As the climate continued to warm to present day conditions, sea level and the water table rose, filling the southern tips of the valleys intersecting Long Island Sound (Sen-Das 2007).

Sen's research is interesting because the watersheds of these stream valleys are sites where a high density of bay formations are found. Sen even sites three of these elliptical depressions throughout her research. The Scuttle hole ponds are a series of elliptical depressions orientating in the NW-SE direction. Interestingly each pond clearly cross cuts a stream valley as seen in the figure 13. Sem categorizes these depressions as kettle lakes formed by the presence of buried ice during the last glacial retreat. She describes how the presence of ice during valley excavation caused such depressions. She argues that the depressions and the dry valleys formed simultaneously after the glacier retreated from Long Island - when there was desert tundra and the environment was periglacial. However, by law of crosscutting relationships. Sen-Das observed that "Tributaries of the valley system seem to have cut right through the Scuttlehole ponds" and this supports the hypothesis that the lake depressions formed after the dry valleys and therefore are younger than the last glacial advance and retreat that occurred 20,000 years ago.

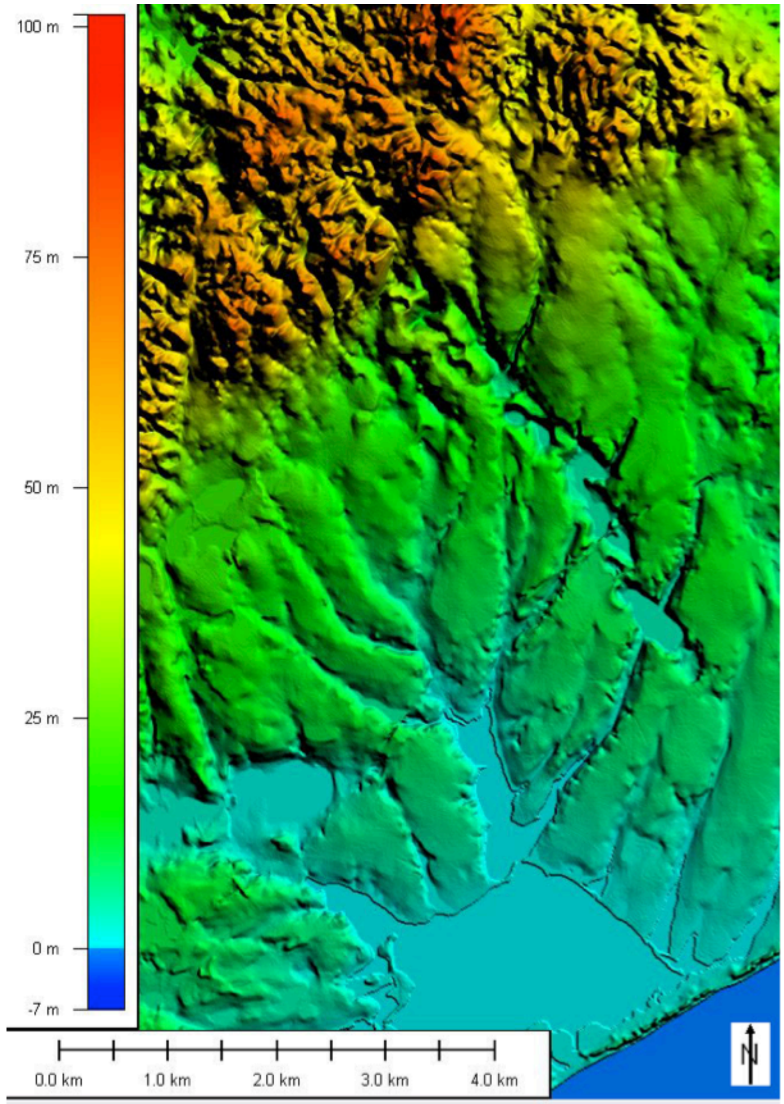

Figure 13: Scuttle hole ponds clearly cross cut parallel dry valley. It is possible that Scuttle hole ponds are Carolina bay formations. (Sen, 2007)

Young Long Island's Post Glacial Permafrost, the Bolling Allerod and the Younger Dryas

Twenty thousand years ago, young Long Island was barren, desert tundra landscape. This cold, dry periglacial climate was characterized by a mean annual temperature of -8°C to -10°C . At this low temperature, frozen ground water temporarily cemented the unsorted compacted till sediments of the North Shore and the progressively finer, sorted sediments of the south shore, in other words, Long Island was in a state of permafrost. Permafrost causes land to be resistant to infiltration and erosion. (Nieter, 1975; Kundic and Hanson, 2006; Denny, 1936). Evidence of post-glacial permafrost is found in almost all parts of Northeast USA extending even further south of Long Island including southern New Jersey. (French et al., 2007) There is debate amongst experts as to when the permafrost began to melt and disappear from the area. Some believe the permafrost melted during the Bolling Allerod

Interstadial event, a sudden warming period that occured 14,600 years ago. (Weaver et al., 2003) However, Mayewski et al. (1993) and Logan (1983) used Greenland Ice Cores to study the ammonia and methane flux and concluded that the Bolling Allerod did not have a significant impact on continents of North America and Europe. Therefore permafrost on Long Island may have lasted until the end of the Younger Dryas, 11,500 years ago. The Younger Dryas is an unexplained rapid cooling event following the Bolling Allerod that began 12,900 years ago. (Weaver et al., 2003). The persistence of permafrost through the end of the younger dryas is supported by the emergence of thermohilous species of trees such as Hemlock, Oak and Pine in the fossil record associated with the climatic warming that ended the Younger Dryas. (Peteet et al. 1994)

Impact Event?
The end of the Pleistocene epoch is characterized by the extinction of megafauna such as the mammoth and the clovis culture, early human ancestors. The cause of this mass extinction is still debated among experts. Researchers have suggested natural vegetation shifts, over-hunting by humans, an impact event, climate changes and plagues, but there is not consensus amoung them yet. (Largent 2008) The Younger dryas cooling event came on abruptly following the Bolling Allerod, 12.9 calendar years ago and lasted approximately 1000 years. (Firestone at el., 2007). It is characterized by a significant drop in temperature in North America, Greenland and Europe. The Clovis came to an end between 12800 and 12925 calendar years ago, as indicated by the presence of "black mats" in rock strata. "Black mats" are dark organic deposits that form a boundary as no evidence of the clovis culture is found above them (Largent 2008). There is contention among researchers over the cause of the younger dryas and the subsequent Pleistocene extinctions. "Prominent scientists have shown that neither human over kill or climate change models adequately account for the patterns found in paleontological and archaeological records of North America" (Eriandson, 2007). "Traditional explainations center on a sudden in-flux of glacial meltwater into the North Atlantic, which would have disrupted the saline density and interfered with established patterns of ocean circulation that contributed to the warming of the Northern hemisphere" (Largent, 2008). Another leading but controversial hypothesis is the Younger Dryas Impact theory. Here the catastrophic cosmic collision of an extraterrestrial object with the Laurentide ice sheet, 12.9 ka years ago, triggered the rapid extinction of many large mammals through direct impact, massive wildfires, terrestrial food reduction, climate change and ecological reorganization. Supporting this hypothesis is the Younger Dryas Event Boundary which is a thin sedimentary layer found in both North America and Europe, containing evidence of an impact such as microspherules, magnetic grains, iridium and carbon rich makers such as vesicular glass carbon. Since the 1980s, iridium has be identified as an impact indicator due to it's presence in the K-T boundary layer. (Kloosterman, 2007) Charcoal and soot in the boundary layer indicate extensive wild fires following the impact. SEM analysis of carbon spherules found in this layer reveal characteristics and compositions similar to spherules found in a crater in Germany (Kennett, 2007) Coinciding with the younger dryas boundary is the Clovis extinction layer. The Prehistoric Clovis culture of North America ceased to exist since the end of the Bolling Allerod. Dissolution and analysis of soot in the Carolina bay area suggests that significant burning occurred in that area 12.9 ka ago. (Wolbach, 2007) Sampling of Clovis ages sites reveal the presence of microscopic nanodiamonds, which are only known to form due to impact events (Largent, 2008).

Recent scientific literature suggests that Carolina bay formations are evidence for the Younger Dryas Impact event. The shallow depressions result from material, blown outward from the impact site, landing across the atlantic coastal plain. The presence of a large amount of soot was documented Carolina Bays a Blackville and Myrtle Beach, South Carolina. Athough this does not prove their connection to an impact event it does indicate that significant burning occurred in those areas

(Wolbach, 2007). Although evidence supporting an impact event is mounting, many scientists doubt it viability due to the lack of a clear impact crater. (Largent 2008).

Conclusion

In 2012, Michael Davias used LiDAR (Light Detection And Ranging) digital elevation maps to identify Carolina bay formations in Maryland, Delaware and New Jersey. Prior to this, and similar to Long Island, bays in these areas were not recognized due to their smaller size and more circular presentation in these states. However, Davias finds that this shape morphology is expected because bay formations become progressively smaller and rounder toward the North. Additionally the major axis of bay orientation changes from north/south in the south to east/west in the north latitude (Fig. 4). Carolina bay formations found on Long Island, New York preserve this pattern of shape evolution towards the North. Thus the shape of the bays found on Long Island, New York most closely resemble bays found in Northern New Jersey. Additionally bays are expected to be smaller and rounder on Long Island and possess an East to West orientation. LiDAR digital mapping technology was successfully used to identify several possible Carolina bay formations in the undeveloped areas of Long Island (Davias, 2012).

Long Island did not exist before the onset of the Wisconsian glaciation. Rather Long Island was deposited during the advance and retreat of at least two glaciations approximately 20,000 years ago. Therefore the bay formations on Long Island must be younger than 20,000 years old.

The shape and size of bay formations on Long Island are consistent with my hypothesis that they would be rounder and smaller. Additionally the orientation of the major axis consistent with Davias hypothesis that the axis line up with a butterfly ejecta pattern and therefore are expected to run West to East in the North.

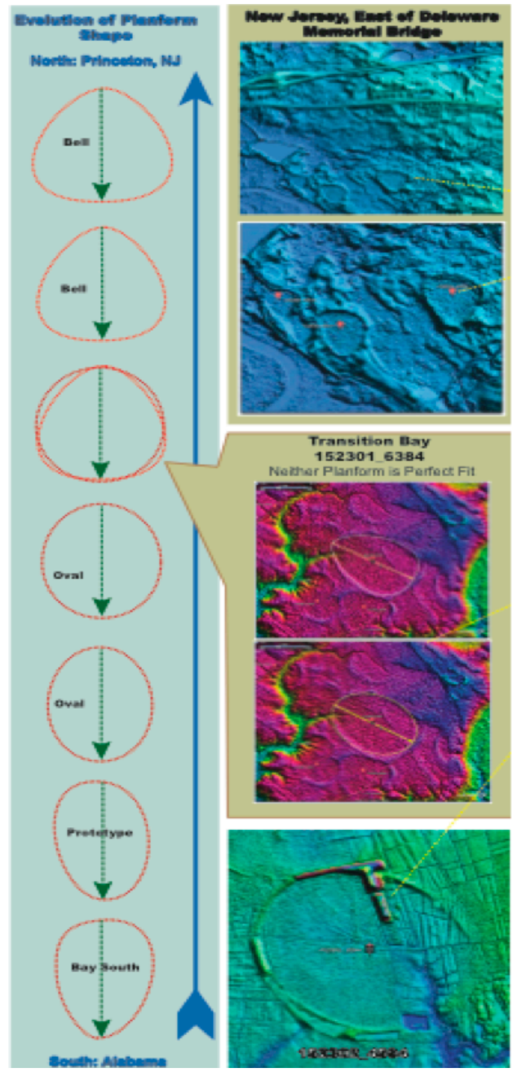

Figure 14: The shape and orientation morphology of Carolina bay formations in New Jersey versus Alabama. Long Island bay more closely resemble bays in New Jersey.

Further research:

Future research is needed to examine bays on Long Island. Research on the composition of the soils and sands in the rims is needed to further link Long Island bays to other bays on the Atlantic Coastal plains. The presence of charcoal within these soils would be interesting as it could yield information about paleo-forest fires and further support the Younger Dryas Impact Theory. Another research effort could focus on documenting more bays toward the north and use glacial retreat data to further narrow the time constraint. Finally I would like to explore the effects of the existence of permafrost on bay formation. Did the permafrost make the ground more resistant to the impact debris, resulting in shallow bays that are hard to see?

Works Cited:

Bennington, J.B., 2003, New observations on the glacial geomorphology of Long Island from a digital elevation model DEM., 10th Conference - Geology of Long Island and Metropoli- tan New York, vol. 10, URL http://pbisotopes.ess.sunysb.edu.lig/conferences/ abstracts/bennington/.

Bliley, D.J., Burney, D.A., 1988. Late Pleistocene climatic factors in the genesis of a Carolina bay. Southeastern Geology 29, 83–101.

Bliley, D.J., Pettry, D.E., 1979. Carolina bays of the eastern shore of Virginia. Soil Science Society of America Journal 43, 558–564.

Blue Marble Geographics. Globbal Mapper ™. Version V14.1. 2012 (online)

Brooks, M.J., Taylor, B.E., Grant, J.A., 1996. Carolina bay geoarchaeology and Holocene landscape evolution on the upper coastal plain of South Carolina. Geoarchaeology 11, 481–504.

Cabe, M., Kelly, M., Schaefer, M., Schwartz, R., Hanson, G. and Benimo↵, A., 2006, Dating Glacial Features in New York's Lower Hudson Valley- The Last Deglaciation of the Eastern Laurentide Ice Sheet, GSA abstracts.

Carver, R.E., Brook, G.A., 1989. Late Pleistocene paleowind directions, Atlantic Coastal Plain, U.S.A. Palaeogeography, Palaeoclimatology, Palaeoecology 74, 205–216.

Davias, Michael. 2012a. Lidar-Dervied Digital Elevation Maps of Maryland, Delaware and New Jersey used to identify Carolina bay landforms. Paper No. 16-11 Northeastern Section-47th Annual Meeting March 18 2012 Hartford Ct

Davias, Michael. 2012b. Cintos Research.Org 2012

Davias, Michal & Jeanette Gilbride. Correlating an impact structure with the Carolina bays. poster. GSA 2010

Denny, C.S., 1936, Periglacial Phenomena in Southern Connecticut, American Journal of Science, vol. 32, pp. 322–42.

Drewberry 2007. 2006 LiDAR Accuracy Report Suffolk County, New York, July 17, 2007

Erlandson, JM . 2007. The Younger Dryas ET Impact Theory and Terminal Pleistocene Mammalian Extintions in North America. AGU Joint Assembly May 22, 2007. Acapulco, Mexico.

Firestone, R.B, et al. 2007. Evidence for an Extraterrestrial Impact Event 12,900 years ago that Contributed to Megafaunal Extinctions and the Younger Dryas Cooling. AGU Joint Assembly May 22, 2007. Acapulco, Mexico.

French, H.M., Demitro↵, M., Forman, S.L. and Newell, W.L., 2007, A Chronology of Late-Pleistocene Permafrost Events in southern New Jersey, Eastern USA, Permafrost and Periglacial Processes, vol. 18, pp. 49–59.

Fuller, M.L., 1914, The Geology of Long Island, US Geological Survey Professional Paper, vol. 82, p. 231.

Gamble, E.E., Daniels, R.B., Wheeler, W.H., 1977. Primary and secondary rims of Carolina bays. Southeastern Geology 18, 199–212.

Grant, J.A., Brooks, M.J., Taylor, B.E., 1998. New constraints on the evolution of Carolina bays from ground penetrating radar. Geomorphology 22, 325–345.

Hanson, G.N., 2005, Glacial Geology of the Stony Brook-Setauket-Port Je↵erson Area, Report., Stony Brook University, http:// pbisotopes.ess.sunysb.edu/ reports/.

Hanson, L., 2006, Fluvial processes and Landforms, Report, http://members.aol.com/ gls210/ streams.htm.

Ivester, A.H., Brooks, M.J., Taylor, B.E., 2007. Sedimentology and ages of Carolina bay sand rims. Geological Society of America Abstracts with Programs 39, 5.

King, C., Mion, L., Pacholik, W. and Hanson, G., 2003, Evidence of Till South of Ronkonkoma Moraine, Conference-abstract, URL http://www.geo.sunysb.edu/lig/ Conferences/abstracts-03/king/king-index.htm.

Kennett, J P. 2007 Evidence for an Extraterrestrial Impact Event 12,900 years ago that Contributed to Megafaunal Extinctions and the Younger Dryas Cooling. AGU Joint Assembly May 22, 2007. Acapulco, Mexico.

Kloosterman, JB. 2007 Correlation of the Late Pleistocene Usselo Horizon (Europe) and the Clovis Layer (North America). AGU Joint Assembly May 22, 2007. Acapulco, Mexico.

Kundic, V. and Hanson, N., 2006, Evidence of Permafrost in Long Island, abstracts, De- partment of Geosciences, Stony Brook University, http://www.geo.sunysb.edu/ lig/ Con- ferences/ abstracts06/ kundic-06.pdf.

Largent, Floyd, 2008. The Clovis Comet. The Mammoth Trumpet. January 2008.

Lewis, R.S., and Needell, S.W. (1987) The Quaternary geology of east-central Long Island Sound: U.S. Geological Survey Miscellaneous Field Studies Map MF-1939-B Pamphlet, p. 1-6

Lewis, R.S., and Stone, J.R. (1991) Late Quaternary stratigraphy and depositional History of the Long Island Sound Basin: Connecticut and New York, Journal of Coastal Research, Special Issue 11, p. 1-23.

Logan, J., 1983, Nitrogen oxides in the troposphere-Global and regional budgets, Journal of Geophysical Research, vol. 88, pp. 10785–10807.

Markewich, H.W., Markewich, W., 1994. An overview of Pleistocene and Holocene inland dunes in Georgia and the Carolinas — morphology, distribution, age, and paleoclimate. U.S. Geological Survey Bulletin 2069, 1–32.

Mayewski, P.A., Meeker, L.D., Morrison, M.C., Twickler, M.S., S.I.Whitlow, Ferland, K.K., Meese, D.A., Legrand, M.R. and J.P.Ste↵ensen, 1993, Greenland ice core 'signal' charac- teristics - An expanded view of climate change, Journal of Geophysical Research, vol. 98, pp. 839–847.

Melton, M., 1957, An Analysis of the Relations Among Elements of Climate, Surface Prop- erties, and Geomorphology, Tech. rep., Dept. of Geology, Columbia University.

Merrill, F. et al., 1902, Metamorphic crystalline rocks of the New York City quadrangle, Tech. rep., Description of the New York City district: United States Geological Survey- Geologic Atlas of the United States, New York City Folio, No. 83, 19 p.(Includes colored geologic map on a scale of 1:62,500).

May, JH; Warne, AG. 1999. Hydrogeologic and geochemical factors required for the development of Carolina Bays along the Atlantic and Gulf of Mexico Coastal Plain, USA. ENVIRONMENTAL & ENGINEERING GEOSCIENCE Volume: 5 Issue: 3 Pages: 261-270

Nieter, W., 1975, A late Wisconsin loess deposit in southeastern Long Island, New York, Master's thesis, Queens College. Department of Earth and Environmental Sciences.

Patton, P.C. and J.M. Kent. 1992. A Moveable Shore: The Fate of the Connecticut Coast. Durham: Duke University Press.

Peteet, D., Daniels, R., Heusser, L., Vogel, J., Southon, J. and Nelson, D., 1994, Wiscon- sinan Late-glacial environmental change in southern New England: A regional synthesis, Journal of quaternary science, vol. 9(2), pp. 151–154.

Poppe, L.J. and C. Polloni (eds). 1998. Long Island Sound Environmental Studies. U.S. Geological Survey Open File Report 98-502 (CD-ROM). For full text see Journal of Coastal Research. 1991. Special Issue No. 11.

Prouty, W.F., 1952. Carolina bays and their origin. Bulletin of the Geological Society of America 63, 167–224.

Pigati, JS (Pigati, Jeffrey S.); Latorre, C (Latorre, Claudio) May 8, 2012.Accumulation of impact markers in desert wetlands and implications for the Younger Dryas impact hypothesis. Proceedings of the national academy of sciences of the United States of America. Volume: 109 Issue: 19 Pages: 7208-

Ridge, J.C., 2011 (Aug. 18), The North American Glacial Varve Project. Retrieved from http://geology.tufts.edu/varves.

Rodriguez, AB; Waters, MN. January 2012. Burning peat and reworking loess contribute to the formation and evolution of a large Carolina-bay basin. QUATERNARY RESEARCH Volume: 77 Issue: 1 Pages: 171-181

Schmitt, K., 2006, More Evidence of Till South of the Ronkonkoma Moraine, 13th Confer- ence - Geology of Long Island and Metropolitan New York, URL http://pbisotopes. ess.sunysb.edu.lig/conferences/abstracts/.

Sen-Das Soma, Hanson, Rasbury. August 2007. Origin and Evolution of the Dry Valleys South of the Ronkoma Moraine. Stony Brook University.

Sirkin, L., 1982, Wisconsinan glaciation of Long Island, New York to Block Island, Rhode Island, in Larson, G.J., Stone, B.D., eds. Late Wisconsinan glaciation of New England:, Kendall/Hunt.

Stolt, M.H., Rabenhorst, M.C., 1987a. Carolina bays on the eastern shore of Maryland: II. Distribution and origin. Soil Science Society of America Journal 51, 399–405.

Stolt, M.H., Rabenhorst, M.C., 1987b. Carolina bays on the eastern shore of Maryland: I. Soil characterization and classification. Soil Science Society of America Journal 51, 394–398.

Stuiver, P. and Messina, P., 1996, The Transient Atlantic Shoreline, Tech. rep., CUNY Earth and Environmental Science, URL http://www.geo.hunter.cuny.edu/bight/coast. html.

Thom, B.G., 1970. Carolina bays in Horry and Marion counties, South Carolina. Geological Society of America Bulletin 81, 783–814.

Weaver, J., Saenko, A., Clark, U. and Mitovica, X., 2003, Meltwater Pulse 1A from Antarc- tica as a Trigger of the Bølling-Allerød Warm Interval, Science, vol. 14, pp. 1709–1713.

Wolbach, W S, et al. 2007 Is There Evidence for Impact-Triggered Fires at the End Pleistocene? AGU Joint Assembly May 22, 2007. Acapulco, Mexico.